

# THE NATURAL HEAT ENGINE

by John C. Wheatley, Gregory W. Swift, and Albert Migliori

**H**eat engines are a compromise between the crisp ideals discussed in thermodynamic textbooks and the clanking, hissing realities of irreversible processes. This compromise produces wonderful machines, such as the automobile engine and the household refrigerator. In designing real devices, the goal is not to approach thermodynamic ideals by reducing irreversibilities but to balance cost, efficiency, size, power, reliability, simplicity, and other factors important to the needs of particular applications.

Simplicity is the most striking feature of a *natural* engine, a reciprocating heat engine with no moving parts. As we will see, the basic operating cycle of the natural engine is so straightforward it can be applied to a wide variety of systems with working media that range from air to paramagnetic disks.

Although the natural engine is new in concept, the underlying thermodynamic principles and processes are shared with conventional engines, such as the Stirling and Rankine engines. To set the stage for natural engines, we will first discuss a few conventional idealized thermodynamic cycles and the practical engines they suggest.

## Conventional Heat Engines and Cycles

In principle, any idealized thermodynamic heat engine cycle is *functionally*

reversible in the sense that it can be made to operate in either of two modes: prime mover or heat pump\* (Fig. 1). In a prime mover, heat flows from high to low temperatures, and the engine converts a portion of that heat to work. In a heat pump, the flows of heat and work are reversed; that is, work done on the engine causes it to pump heat from low to high temperatures. Few practical engines are functionally reversible. The internal combustion engine is a prime mover only; the household refrigerator is a heat pump only: neither engine is ever operated in both modes,

Figure 1 shows how the first and second laws of thermodynamics place an upper limit on the *efficiency of a prime mover* (the fraction of the heat input converted to work). The efficiency of a *thermodynamically* reversible cycle—that is, one in which all parts of the system are always in thermodynamic equilibrium—is equal to that upper limit. (One statement of the second law of thermodynamics is that all reversible engines operating between the same two temperatures have the same efficiency.) Figure 1 also shows the upper

---

\*A *prime mover* is often called an *engine* and a *heat pump* a *refrigerator*. Here we use the term *engine* to denote both *thermodynamic functions*, and our use of the term *heat pump* includes the *refrigerator*. Strictly speaking, however, the purpose of a *heat pump* is to reject heat at the higher temperature, whereas the purpose of a *refrigerator* is to extract heat at the lower temperature.

limit for the *coefficient of performance (C. O. P.) of a heat pump* (the amount of heat rejected at the higher temperature per unit of work). Both theoretical limits depend only on the temperatures involved.

**Carnot.** The most fundamental engine cycle operating between two temperatures is the functionally and thermodynamically reversible cycle propounded by Sadi Carnot in 1824. The cycle consists of alternating adiabatic and isothermal steps (Fig. 2). During an adiabatic step, no heat flow occurs ( $Q = 0$ ) and entropy ( $\int dQ/T$ ) remains constant. Thus any flow of work causes a corresponding change in the temperature of the working medium. During an isothermal step, the temperature remains constant, and flows of entropy, work, and heat occur.

In the Carnot cycle, the entropy change of one isothermal step exactly balances the entropy change of the other isothermal step. Over a complete cycle, no entropy is generated. If an engine could be made to follow a Carnot cycle, its efficiency would equal the theoretical upper limit given in Fig. 1. Although the upper limit applies to any reversible engine, this efficiency is usually called the Carnot efficiency.

Building an engine that approximates a Carnot cycle requires that all processes in its cycle are carried out very near equilibrium. If not, the resulting irreversibilities due to temperature and pressure gradients generate entropy and cause a loss of efficiency. For example, the



The release of acoustic energy by a simple natural heat engine, the Hoffer tube, made evident by the white plume at the upper end. The device consists of a two-piece copper tube, closed at the bottom, and a short set of fiber glass plates that run parallel to the tube's axis in the region of the flanges. The acoustic energy results spontaneously when a temperature gradient is applied across the plates. In this case, the gradient was produced by holding one end of tube tube while immersing the other end (frosted) in liquid nitrogen

temperature differences across the heat exchangers that move heat in or out of the engine are frequently a source of irreversibility that greatly cuts efficiency. (See "The Fridge" for a quantitative accounting of this and other losses in a practical heat pump.)

Although one may approach near-equilibrium conditions by designing the engine so as to reduce these gradients, the end result is a very slow cycling of the engine and a very low power output. An important point (originally made by F. L. Curzon and B. Ahlborn and generalized by S. Berry, J. Ross, and their collaborators) is that Carnot-like cycles operating between two temperatures with imperfect heat exchangers have quite different efficiencies depending on whether work per cycle or power is being maximized. Real engines, especially high-speed reciprocating engines, cannot approximate Carnot's cycle closely,

**Stirling.** The Stirling *engine*, invented in 1816 by the Reverend Robert Stirling some eighteen years before Carnot's ideas were published and originally called the hot-air engine, is a reciprocating engine that is functionally reversible and, in principle, thermodynamically reversible. The ideal Stirling *cycle* has the Carnot efficiency. From a practical standpoint, implementing the Stirling cycle suffers from some of the problems of implementing the Carnot cycle. However, the introduction of a second thermodynamic medium provided the means by which high-speed Stirling engines of good efficiency could be built.

The Stirling *cycle* (the solid black curve in Fig. 3) differs from the Carnot cycle in that the adiabatic steps are replaced with steps that are reversible by virtue of being *locally* isothermal. This type of cycle is achieved by using *two* thermodynamic media. The first is the working fluid, which typically can be either a gas or a liquid. (There are Stirling cycles that use solids, but we do not discuss them here.)

*continued on page 6*

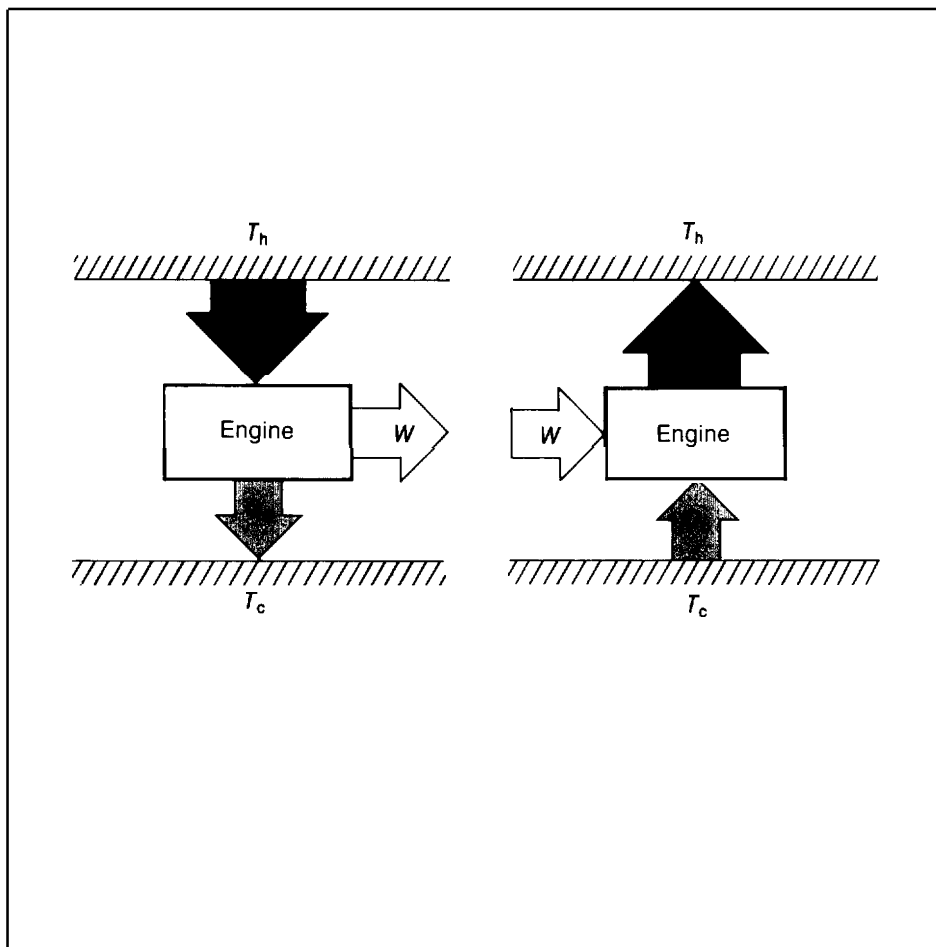
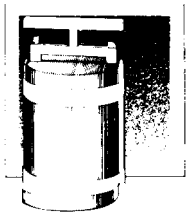


**Fig. 1.** (a) A heat engine operating as prime mover converts some of the heat that is flowing from a hot temperature  $T_h$  to a cold temperature  $T_c$  into work. The first law of thermodynamics tells us that  $Q_h$ , the heat that passes into the engine at the hot temperature, equals  $Q_c$ , the heat put back into the environment at the cold temperature, plus  $W$ , the work done by the engine. The second law tells us that the entropy per cycle generated by the system must be positive or, at best, zero. Since the engine is assumed to be in a steady state, the entropy change in the environment due to the heat flow out of the engine,  $Q_c/T_c$ , is greater than or equal to that due to the heat flow into the engine,  $Q_h/T_h$ . Together, these two laws give an upper

limit for  $W/Q_h$ , the efficiency of the engine. Note that a prime mover can only approach its highest efficiency of unity when  $T_c \ll T_h$ . (b) In a heat engine operating as heat pump, all flows of heat and work are reversed. Thus work done on the engine causes it to draw heat out of the environment at the cold temperature and place it into the environment at the hot temperature. Consideration here of the first and second laws leads to an upper limit on the coefficient of performance (C.O.P.),  $Q_c/W$ , which is the reciprocal of the efficiency of a prime mover. (For a refrigerator, the C.O.P. is better defined as the ratio of the heat extracted at the lower temperature to the work done on the machine, that is,  $Q_c/W$ .)

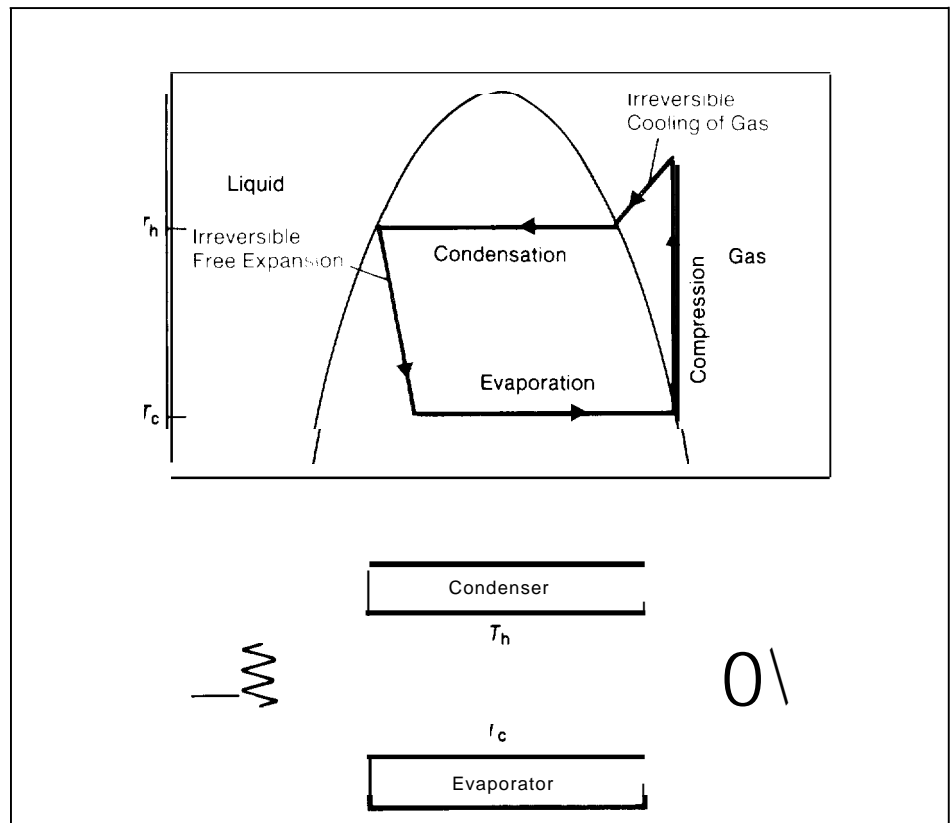


# The Fridge

The basis for the household refrigerator is the Rankine cycle, which, as shown in the figure, duplicates a portion of the Carnot cycle in that it has one adiabatic step and two isothermal steps. A key feature of this cycle is a phase change in the working fluid, and the two isothermal steps correspond to condensation of the fluid at  $T_h$  and evaporation at  $T_c$ . Also, the engine operates with continuous flow rather than by reciprocating: the working fluid cycles through its various thermodynamic states by being forced around a closed loop.

This cycle has intrinsic irreversibilities associated with the free expansion of the liquid and the cooling of the gas to the temperature at which condensation occurs. Thus one expects the Rankine cycle to have less than ideal Carnot efficiency—even before accounting for such losses as those due to temperature differences at the heat exchangers. Nevertheless, Rankine engines remain the design of choice in many applications because they are simple and powerful. Many refrigerators will run thirty years with little or no maintenance, and overall cost is low.

The Rankine cycle can also be used in an air-to-air heat pump. Table 1 illustrates the effects of various irreversibilities on the coefficient of performance for such a pump—one designed to keep a house at 20°C when outside air is 5°C so that, ideally,  $T_h - T_c$  is 15°C and the Carnot coefficient of performance is 19.5. The largest drop in the the estimated coefficient of performance occurs when ideal heat exchangers are replaced by practical heat exchangers—ones both small enough to get through the door of a house and cheap enough to cost less than the house. A small, cheap heat exchanger can only transfer large amounts of heat if a large temperature difference occurs across it. The net effect in our example is that the



The Rankine cycle, used in the household refrigerator, is based on a liquid-gas phase change. The cycle is shown here superimposed on the phase diagram for the working fluid; a schematic of the heat pump is also shown. The Rankine cycle resembles the Carnot cycle in that there are two isothermal

steps and, on the compression side, an adiabatic step. The two parts of the cycle (shown in red) that differ from the Carnot cycle—the cooling of the gas at constant pressure to the condensation temperature  $T_h$  and the free expansion of the liquid—are intrinsically irreversible. A

**Table 1**

**Losses in the coefficient of performance (C. O. P.) due to irreversibilities for an air-to-air heat pump (adapted from *Heat Pumps* by R. D. Heap, 1983).**

Cycle	Irreversibilities	$T_c$ (°C)	$T_h$ (°C)	C.O.P.
Carnot	none	5	20	19.5
Carnot	real heat exchangers	-5	45	6.4
Rankine	real heat exchangers, intrinsic irreversibilities	-5	45	5.1
Rankine	real heat exchangers, intrinsic irreversibilities, compressor losses	-5	45	4.0
Rankine	real heat exchangers, intrinsic irreversibilities, compressor losses, miscellaneous	-5	45	3.0

temperature difference.  $T_h - T_c$  of the working fluid increases from 15°C to 50°C, causing the coefficient of performance for the Carnot cycle to drop from 19.5 to 6.4.

The C.O.P. drops to 5.1 when one takes into account the intrinsic irreversibilities of the Rankine cycle. Further decreases occur because of losses in the compressor

(due to friction and the imperfect conversion of electrical power to shaft power) and miscellaneous losses (such as power to run the fans, the thermostat, and the controls). The final C. O.P. for a practical, operating Rankine heat pump is 3.0, more than a factor of 6 lower than the C.O.P. for an ideal engine. ■

continued from page 4

The working fluid is displaced at constant volume through a *regenerator* containing the second medium, which is typically a solid. The second medium can be metal plates or just the walls of the vessel, but its heat capacity should be large compared to that of the working fluid. A small temperature gradient exists along the length of the regenerator, the total temperature change being the temperature difference between the hot and cold heat exchangers at the ends of the regenerator. If we ensure good thermal contact between the two thermodynamic media (say by making the distance between any fluid element and its adjacent regenerator plate small enough), the fluid can temporarily store heat in the regenerator and recover it later under nearly reversible isothermal conditions. Of course, the steeper the gradient along the regenerator or the faster the displacement of the working fluid through the heat exchangers and the regenerator, the greater the irreversible losses.

During one part of the cycle, fluid enters the cold end of the regenerator, picks up heat from the second medium, and exits hot. During another part of the cycle, fluid enters the hot end of the regenerator, deposits heat in the second medium, and exits cold. The net heat stored in the second medium over a complete cycle is zero (provided, as is the case for an ideal gas, the specific heat of the fluid does not depend on pressure). The regenerator, therefore, enables us to change the temperature of the working fluid from the temperature of the hot reservoir  $T_h$  to the temperature of the cold reservoir  $T_c$  and back again without the adiabatic expansions and compressions of the Carnot cycle. In other words, *locally* isothermal reversible steps have replaced the adiabatic reversible steps for changing the temperature of the working fluid. As a result, the efficiency of the Stirling cycle is the same as that of the Carnot cycle.

But what about the Stirling engine? Typically, Stirling engines do *not* follow a Stirling cycle but rather follow an

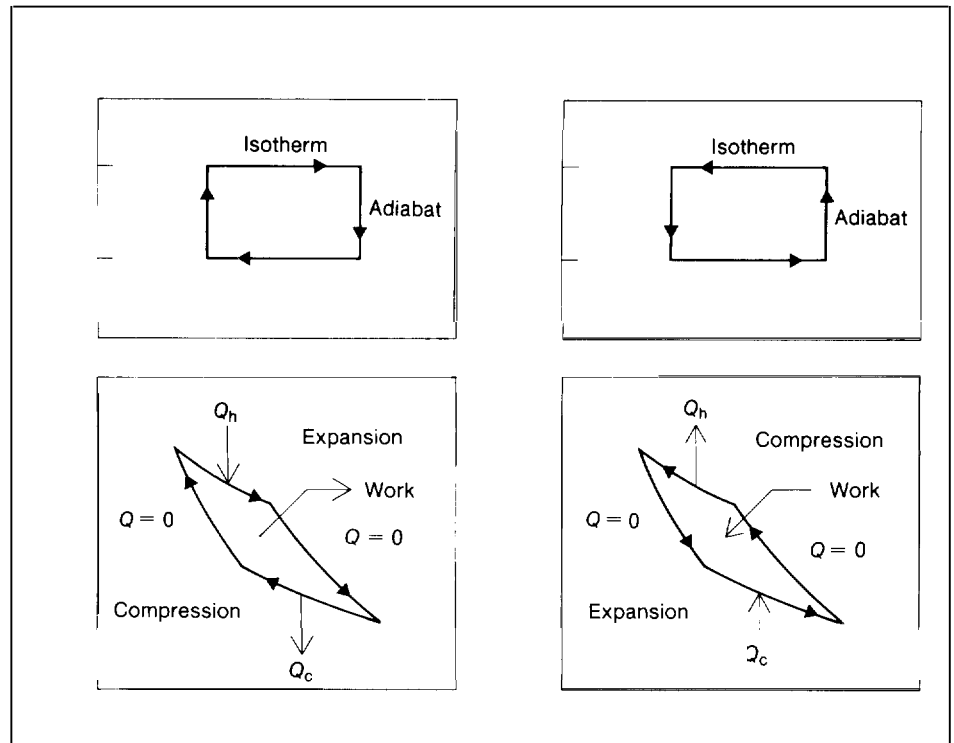


**Fig. 2. Temperature-entropy and pressure-volume diagrams for the prime-mover and heat-pump modes of a Carnot cycle. When the engine is operating as a prime mover, the first part of the expansion stroke is the addition of heat to the engine at  $T_h$ . Because this process is isothermal, the heat energy is used to expand the working medium and do work on the surroundings. In the second step, further expansion occurs adiabatically, that is, with *no* addition of heat or change in entropy. Because**

adiabatic pseudo-Stirling cycle (the dashed curves in Fig. 3), This confusing nomenclature is illustrative of the compromises made between the concept of a thermodynamic cycle and the construction of an operating engine. Unfortunately, because the same person's name can become attached to both the cycle and the engine, confusion abounds,

What changes the Stirling cycle to a pseudo-Stirling cycle is related to the tem-

work continues to be done by the fluid, the temperature of the medium must drop. The third step is isothermal compression in which heat is rejected from the engine to the lower temperature  $T_c$  and the entropy drops. Finally, an adiabatic compression raises the temperature of the medium. The Carnot cycle for a heat pump is just the reverse of that for a prime mover. The area enclosed by the pressure-volume diagrams equals the net work done by or on the engine in a full cycle.

perature of the working fluid at the heat exchangers. An adiabatic compression warms the fluid prior to its displacement through the hot heat exchanger and into the regenerator, and, at the other end of the cycle, an adiabatic expansion cools the liquid prior to its displacement in the opposite direction. These adiabats partially replace the isotherms of the original cycle, necessitating extension of the constant-volume displacement steps.

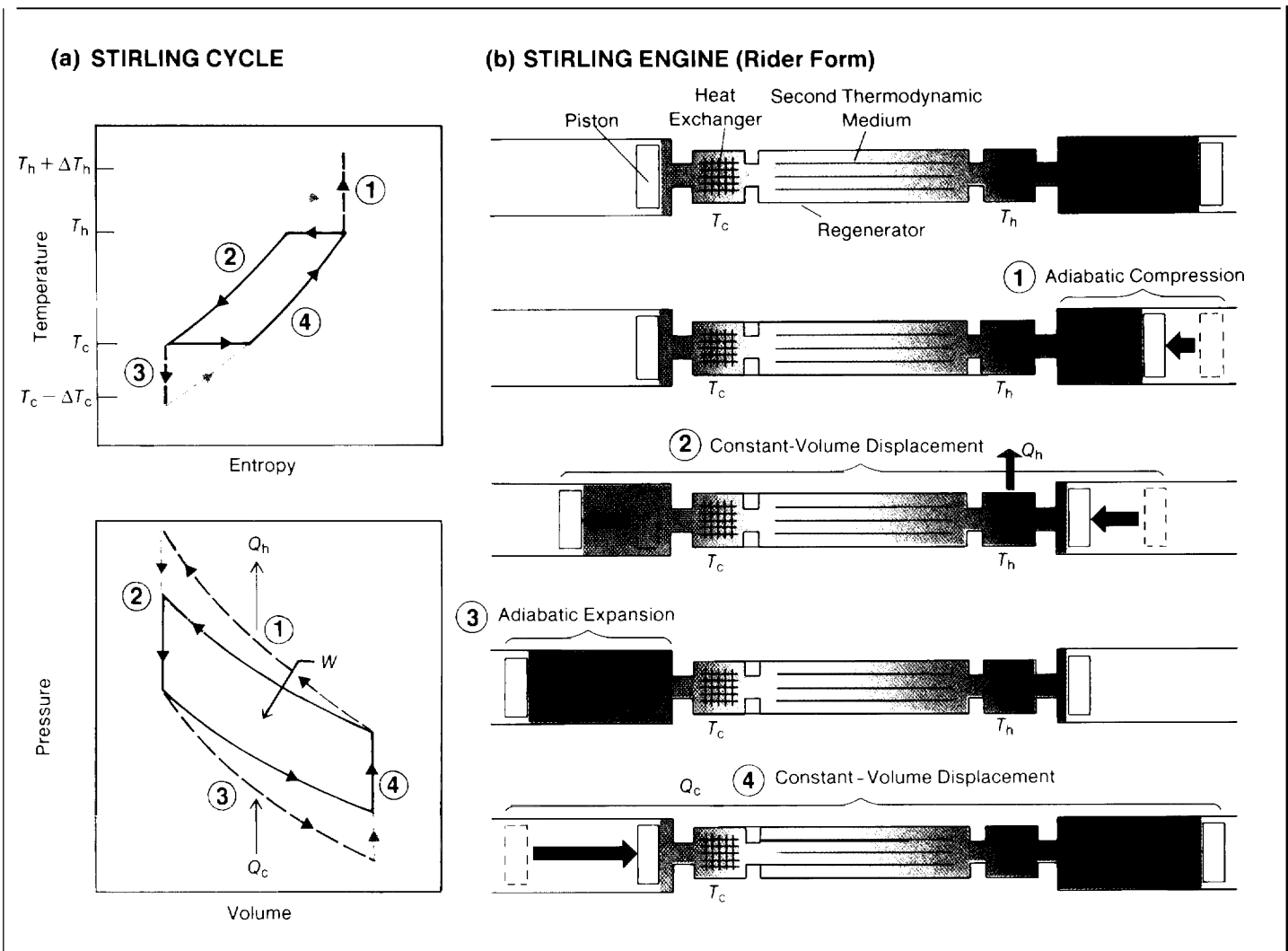


Fig. 3. (a) The ideal Stirling heat-pump cycle (black) consists of isotherms and constant-volume steps. The adiabatic pseudo-Stirling cycle replaces the isotherms with adiabats and extensions of the constant-volume displacement steps (dashed curves). It is the pseudo-Stirling cycle that frequently serves as the basis for practical Stirling engines. (b) One variation (the Rider form) of a Stirling engine following the adiabatic pseudo-Stirling cycle. All such engines are based on the ideal of local isothermal steps made possible through

the use of a second thermodynamic medium in the regenerator. The first step of the cycle depicted here is adiabatic compression in the cylinder on the right that raises the temperature of the fluid above  $T_h$ . In the second step, both pistons move, displacing the fluid to the left. The heat  $Q_h$  generated by the compression is rejected in the heat exchanger on the right. Because of the small longitudinal temperature gradient and good lateral thermal contact along the regenerator, heat is transferred between the two media under essentially

isothermal conditions, cooling the fluid from  $T_h$  to  $T_c$ . In the third step, adiabatic expansion cools the fluid in the left cylinder. Constant-volume displacement of the fluid to the right then causes heat  $Q_c$  to be drawn in at the left heat exchanger and the heat stored in the second medium during step 2 to be returned to the fluid. Irreversibility occurs at the beginning of both constant-volume displacements (dashed red in part (a)) when the fluid at one temperature contacts the heat exchanger at a different temperature.

Since the above alterations introduce intrinsic irreversibilities, the maximum efficiency possible for the pseudo-Stirling cycle is lower than that for the true Stirling cycle. In particular, fluid that has been warmed by adiabatic compression (and thus raised to temperature  $T_h + \Delta T_h$ ) is pushed into the hot heat exchanger during the displacement step, where it makes thermal contact irreversibly with the exchanger at temperature  $T_h$ . The same type of irreversibility occurs in the other heat exchanger after the adiabatic expansion step. Such effects are departures from the ideal of locally isothermal conditions.

Although a Stirling engine is not as simple conceptually as a Carnot engine, practical Stirling engines that operate at moderately high frequencies can indeed be built. As before, other irreversible losses occur because there must be significant temperature differences to drive heat through the heat exchangers. Also, if the working fluid is a liquid (see "The Liquid Propylene Engine"), an additional type of irreversibility arises: the specific heat of a liquid is pressure-dependent, making the recovery of heat in the regenerator imperfect. This irreversibility is not an intrinsic feature of the cycle but is a material property that cannot be avoided. As such, it is of a more fundamental nature than the limitation, say, of the heat exchangers.

*Phasing* of the various moving parts in a heat engine is another factor necessary to its operation. Although the engine depicted in Fig. 3 is a heat pump, if the phasing of the two pistons is altered so that expansion occurs on the hot-temperature side when most of the fluid is hot and compression occurs on the low-temperature side when most of the fluid is cold, heat flow will be reversed and the engine will become a prime mover. As we shall see, both phasing and the second thermodynamic medium are of key importance in natural heat engines also, although there are significant differences in the way in which the second medium is used.

**Internal Combustion.** One way to cir-

cumvent the loss of efficiency from irreversibilities at the heat exchangers is to generate the heating or cooling effects *inside* the engine rather than outside. In 1893 Rudolf Diesel envisioned such an engine and, in fact, intended it to follow a Carnot cycle of adiabats and isotherms. His idea was to provide the heat for the isothermal expansion by burning coal dust that was injected into the engine at just the proper rate to maintain isothermal conditions. Cooling for the isothermal compression was to be provided by spraying water into the chamber. So far, no one, including Diesel, has been able to implement this cycle, and we are once again confronted with confusing nomenclature: the modern Diesel engine does not follow the Diesel cycle,

The idea of internal combustion, of course, survived, and modern Diesel engines work very well indeed. But internal combustion introduces new practical irreversibilities. For example, the addition and burning of the fuel in a typical piston engine causes differences between the pressure and temperature in the cylinder at the end of the cycle and at the beginning. A considerable irreversible loss occurs as heat and pressure are vented in the exhaust. Thus, internal combustion engine cycles differ from the Carnot and Stirling heat engine cycles described earlier in that the working medium is not returned to its original state.

Nevertheless, the use of phased and controlled internal combustion eliminates the problem of bringing heat in through a firewall. The diesel and gasoline internal combustion engines are used today because they are simple, both in principle and in practice, their power density is very high, and their efficiency is relatively good, sometimes very good. Practical diesel engines approach a level of efficiency in which the useful work is nearly half the heating value of the fuel.

**Otto and Brayton.** Two common heat engine cycles that will help illuminate the characteristics of a natural engine are the

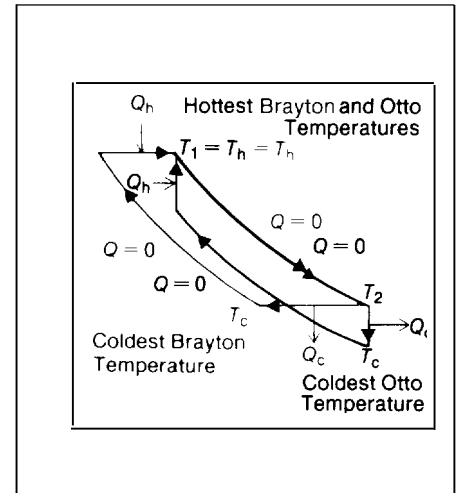


**Fig. 4. The Otto (black) and Brayton (red) heat engine cycles, which consist of two adiabatic steps that alternate with two nonadiabatic steps—the latter steps being the addition or removal of heat at constant volume in the Otto cycle and at constant pressure in the Brayton cycle. Only the prime mover mode is shown. Note that for both cycles the highest temperature  $T_1$  equals the temperature  $T_n$  at the upper extreme of the adiabatic expansion step but that the coldest temperature  $T_c$  is lower than the temperature  $T_2$  at the lower extreme of the adiabatic expansion step.**

Otto cycle (black curve in Fig. 4) and the Brayton cycle (red curve). Each of these cycles, both of which are typically implemented irreversibly, has two adiabatic steps and two nonadiabatic steps. In the Otto cycle, the nonadiabatic steps are the addition and removal of heat at constant volume; in the Brayton cycle, these steps are carried out at constant pressure.

If the working fluid is an ideal gas, both cycles have the same efficiency  $\eta$  given by

$$\eta = 1 - \left( \frac{V_1}{V_2} \right)^{\gamma-1} \quad (1)$$

where  $\gamma$  is the ratio of the specific heat at constant pressure to that at constant vol-

ume. What is interesting about this formula is that efficiency for these cycles is determined by *geometry* (the ratio  $V_1/V_2$  of the volumes at the extremes of the adiabatic expansion step) and by a *fluid parameter*  $\gamma$  but *not* by  $T_h$  and  $T_c$ , the temperatures of the hot and cold reservoirs.

Since for an ideal gas the quantity  $TV^{\gamma-1}$  is constant along an adiabatic path, efficiency can also be expressed in terms of the temperatures,  $T_1$  and  $T_2$ , at the extremes of the adiabatic expansion step:

$$\eta = 1 - \frac{T_2}{T_1}. \quad (2)$$

The diagrams for the Otto and Brayton cycles show that in both cycles  $T_1$  equals  $T_4$  but  $T_2$  is lower than  $T_3$ . This difference is due to further cooling, after the adiabatic expansion step, along a nonadiabatic step (removal of heat at constant volume in the Otto cycle and at constant pressure in the Brayton cycle). If we now examine the limiting case of zero heat transferred during the nonadiabatic steps, we see that  $T_2$  approaches  $T_c$  and the efficiency approaches the Carnot efficiency. Of course, at the same time, the area enclosed by either cycle, and thus the work output, shrinks to zero.

We will find that all of these features of the Otto and Brayton cycles have counterparts in the natural engine.

## The Natural Heat Engine

One guiding principle in the development of most heat engine cycles has been to minimize irreversibilities because they generate entropy and decrease efficiency. In the development of practical engines, however, irreversibilities are often deliberately introduced to increase power, decrease maintenance, or simplify design and manufacture, enabling one, for example, to build small engines, or high-speed reciprocating engines, or cheap engines.

On the other hand, irreversibilities play

a more fundamental role in the natural heat engine. Rather than tolerating irreversibilities for the sake of expediency, the natural heat engine takes advantage of them. For example, heat conduction across a temperature gradient is central to the operation of a natural heat engine known as the acoustic heat engine. Without this irreversibility, the engine would not work. The result of such an approach is a significant leap in simplicity and, for certain applications, a leap in power and efficiency.

Thus, whereas engines that approximate, say, the Stirling cycle are intrinsically reversible (though possibly irreversible in practice), natural heat engines are intrinsically irreversible—they cannot work if irreversibilities are eliminated. Nature abounds with useful irreversible processes, so, for the sake of a short, appropriate, and easily remembered name, we call intrinsically irreversible engines *natural engines*.

**Acoustic Engines.** Work in Los Alamos on natural engines began with an acoustic heat-pumping engine. Our work, however, was preceded by two conceptually related devices, which we will describe without, for the moment, explaining their somewhat surprising behavior.

W. E. Gifford and R. C. Longworth invented what they called a pulse tube (Fig. 5a). Part of this closed tube was fitted with a set of Stirling-type regenerator plates intended to promote locally isothermal processes along their length, and part of the tube was left empty. Pulses were produced at the regenerator end of the tube by switching between high- and low-pressure gas reservoirs at a rapid rate (1 hertz). The extreme inner end of the regenerator plates got very cold, whereas a heat exchanger withdrew heat at the empty end of the tube. The pulse tube demonstrated the pumping of heat with acoustic energy in the presence of a second thermodynamic medium.

The other significant precursor to our work, and one of which we were initially

unaware, was the half-wave resonator of P. Merkli and H. Thomann (Fig. 5b). In this apparatus, a piston drives pressure fluctuations in air at nearly half-wave resonance in a simple closed tube. Merkli and Thomann observed that the center of the tube *cooled*, whereas the ends of the tube *warmed*. At first, these results seem surprising. Naively, one might expect heating everywhere rather than cooling in one region. Further, the cooling occurred in the center, which, at a quarter of an acoustic wavelength, is coincident with a maximum, or antinode, in acoustic velocity and thus where one would surely expect a warming due to viscous scrubbing of the air on the walls.

The first acoustic heat pump built at Los Alamos used a speaker at one end of a closed tube to drive the acoustic resonance and has a stack of fiber glass plates positioned toward the opposite end (Fig. 5c). The plates constitute a second thermodynamic medium but not a Stirling-like regenerator because they are spaced so far apart that locally isothermal conditions do *not* prevail. With such an arrangement, it is easy to produce a 100-centigrade-degree temperature difference across a 10-centimeter-long stack of plates in only a minute or so.

Subsequently, Tom Hofler built a device (opening photograph and Fig. 6) to show his Ph.D. candidacy committee at the University of California, San Diego. The device, which we call the Hofler tube, consists of a quarter-wave acoustically resonant metal tube closed at one end and a stack of fiber glass plates that run parallel to the axis of the tube. Short copper strips glued at each end of each fiber glass plate provide heat exchange by making contact with two flanges encircling the tube.

If the closed end of the tube is heated, say by holding it in a warm hand, and its open end is cooled by dipping it in liquid nitrogen, the resulting steep temperature gradient causes the air in the tube to vibrate, and the person holding the tube will feel his or her whole arm begin to shake. When the tube is removed from the

liquid nitrogen, the sound of the acoustic oscillations is very intense. Peak-to-peak pressure oscillations at the closed end have been found to be as high as 13 per cent of the atmospheric pressure! Thus, the tube operates as a prime mover, and heat is converted to acoustic work.

How do this and other acoustic engines work? The Hofler tube is the grandchild of the Sondhauss tube, famous in thermoacoustics and explained qualitatively by Lord Rayleigh over a hundred years ago. Theoretical understanding of these and related devices has been promoted by Nikolaus Rott in a series of papers published over the last fifteen years. The same conceptual foundation can be used to understand quantitatively not only the Hofler tube but the other acoustic devices mentioned above as well.

As mentioned before, an important factor in the operation of traditional engines is phasing: pistons and valves have to move with correct relative timing for the working medium to be transported through the desired thermodynamic cycle. The natural engine contains no obvious moving parts to perform these functions, yet the acoustic stimulation of heat flow and the generation of acoustic work point to some type of cycling, or timed phasing of thermodynamic processes.

The key to phasing in natural engines is the presence of two thermodynamic media. In the Hofler tube, gas was the first medium, the fiber glass plates were the second. Consider a parcel of gas that moves back and forth along the plates at the acoustic frequency. As it moves, the parcel of gas will experience changes in temperature. Part of the temperature changes come from adiabatic compression and expansion of the gas by the sound pressure and part as a consequence of the local temperature of the plate itself. The heat flow from gas to plate that occurs as a consequence of these temperature differences does not produce *instantaneous* changes. Rather a *thermal lag* in the heat flow between the two media creates the phasing between temperature and motion

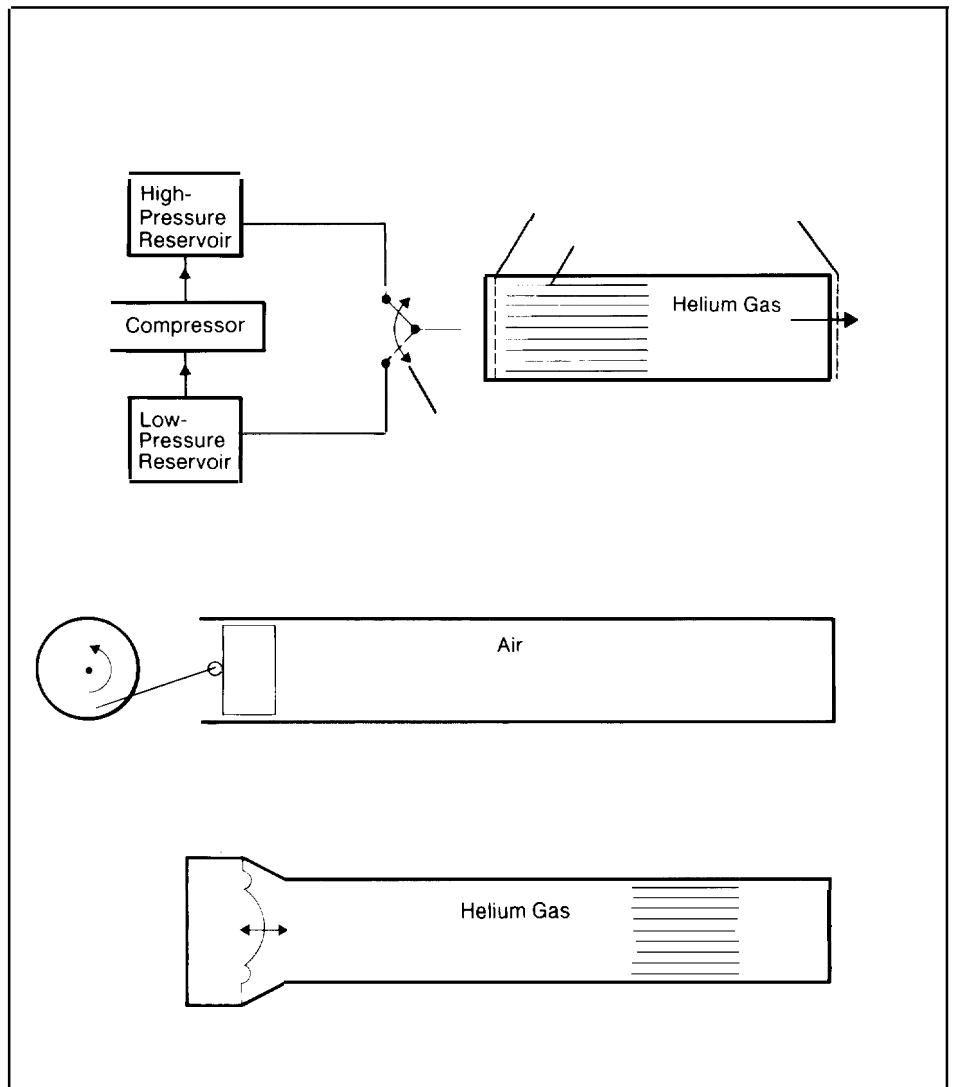


**Fig. 5. (a) At the left end of the Gifford and Longworth pulse tube, pressure pulses in a gas are generated at 1 hertz (Hz) by switching between high-pressure (5 bars) and low-pressure (1 bar) reservoirs. In conjunction with two second thermodynamic media (a Stirling-type regenerator and the walls of the open section of the tube), the pulses cause heat to be pumped from the middle of the tube to the far right. (b) The half-wave resonator heat pump of Merkli and Thomann is a simple closed tube whose acoustic resonance is**

**driven on the left by a reciprocating piston. Contrary to one's intuition, the center of the tube, where the acoustic velocity is greatest, cools rather than warms. (c) The first acoustic heat pump built at Los Alamos contains a stack of fiber glass plates and helium gas as the working fluid. The quarter-wave acoustic resonance is driven on the left by a speaker. The stack acts as a second thermodynamic medium but is not a Stirling-like regenerator because the wide spacing of the plates does not promote locally isothermal conditions.**

that is needed to drive the engine through a thermodynamic cycle. This is why a natural but irreversible process—heat flow across a temperature difference—is intrinsic to the operation of the engine.

An interesting contrast exists between the Stirling engine and natural engines. In the Stirling engine, good thermal contact between the working fluid and the second medium helps ensure reversible operation and high efficiency. In the acoustic heat engine, *poor* thermal contact is necessary to achieve the proper phasing between temperature and motion of the working fluid.

One additional condition is important to the operation of the acoustic heat engine: thermodynamic symmetry along the direction of relative motion must be broken. The concept of thermodynamic symmetry is fundamental. It is conceptually simple. In the natural engine, the two thermodynamic media are undergoing reciprocating relative motion along one direction and are interacting thermodynamically in a direction transverse, or laterally, to the motion. If the lateral interaction does not change as we move in the direction of relative motion, we say there

is thermodynamic symmetry. But if the lateral interaction changes with the longitudinal coordinate, the symmetry is said to be broken. Where the symmetry is broken there is always some thermodynamic consequence, such as a change of temperature or a heat flow to an external reservoir.

Thermodynamic symmetry can be broken in a variety of ways. For example, in the heat pump depicted in Fig. 5c, it is broken *geometrically* at the longitudinal ends of the fiber glass plates. In our description of some variable stars as natural engines, it is broken by changes in opacity that alter the effective thermal contact between the stellar matter and the radiation field. It can also be broken *dynamically* by, for example, nonlinear localization of the acoustic energy in the primary medium.

The dramatic effects of breaking thermodynamic symmetry can be shown experimentally by fixing several thermocouples to the central plate of a simple acoustic heat pump (Fig. 7). When the acoustic driver or speaker is turned on, the temperature of thermocouples at the ends (where thermodynamic symmetry is

broken) changes rapidly and by large amounts, whereas the temperature of other thermocouples further in along the plates changes only by small amounts. In an acoustic natural engine, the heat exchangers are, of course, located at positions where thermodynamic symmetry is broken.

Before explaining in more detail the operation of the acoustic heat engine, we summarize by pointing out that *all* natural heat engines possess the following elements:

- two or more thermodynamic media in reciprocating relative motion,
- an irreversible process that causes phasing of a thermodynamic effect with respect to the motion, and
- broken thermodynamic symmetry along the direction of relative motion.

**The Cycle.** Figure 8 displays the cycles of an acoustic engine serving as prime mover and as heat pump and also follows a typical parcel of gas as it oscillates alongside one of the fiber glass plates. In a real

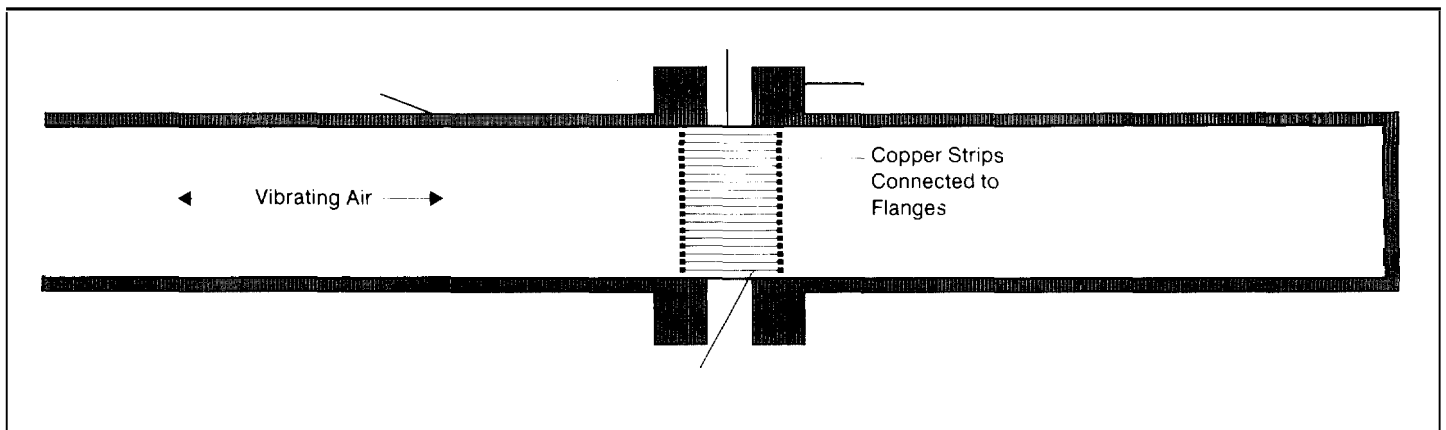


**Fig. 6. The Hofler tube, a simple acoustic prime mover that consists of two thermodynamic media—air and fiber glass plates—inside a quarter-wavelength acoustically resonant tube closed at one end. If a steep tempera-**

**ture gradient is applied across the plates, the air in the tube vibrates strongly. The plates are 1.65 cm long, 0.38 mm thick, and spaced 1 mm apart. The stack of plates, here seen from the side, is placed about midway in the**

**tube. Thermal contact between the plates and the tube at both ends of the stack is provided by thin copper strips that run along the longitudinal edges of each plate and into the thick encircling copper flanges.**

acoustic engine, the oscillations are sinusoidal, producing elliptical cycles. For simplicity we consider square-wave, or articulated, motion so that the basic thermodynamic cycle can be pictured as consisting of two reversible adiabatic steps and two irreversible constant-pressure steps, as in the Brayton cycle.

Just as in the Stirling engine, relative phasing of motion (steps 1 and 3 in Fig. 8) and heat transfer (steps 2 and 4) determines whether the acoustic engine is a prime mover or a heat pump. In the Rider form of a Stirling engine, phasing is effected externally by altering the order in which pistons are moved. In an acoustic engine, however, phasing is a result of the natural time delay in the diffusion of heat between the two thermodynamic media. The sign of the relative phasing, and thus the mode of the natural heat engine, is determined by the magnitude of the temperature gradient along the fiber glass plates—a remarkable quality and a substantial gain in simplicity.

During the compressional part of the acoustic standing wave, the parcel of gas is both warmed and displaced along the plates. As a result, two temperatures are important to that parcel: the temperature of the gas after adiabatic compressional warming and the temperature of the part of the plate next to the gas parcel after compression (and displacement). If the temperature of the gas is *higher* than that of the plate, heat will flow from the gas to the plate. If the temperature of the gas is *lower* heat flows in the opposite direction from plate to gas. Both heat and work flows can thus be reversed and the engine switched between functions by altering the size of the temperature gradient. A zero or low gradient is the condition for a heat pump: a high gradient is the condition for a prime mover. This engine is intrinsically irreversible but, *functionally* reversible.

The gradient that separates the two modes is called the *critical* temperature gradient  $\nabla T_{crit}$ . For this gradient, the temperature change along the plate just matches the temperature change due to

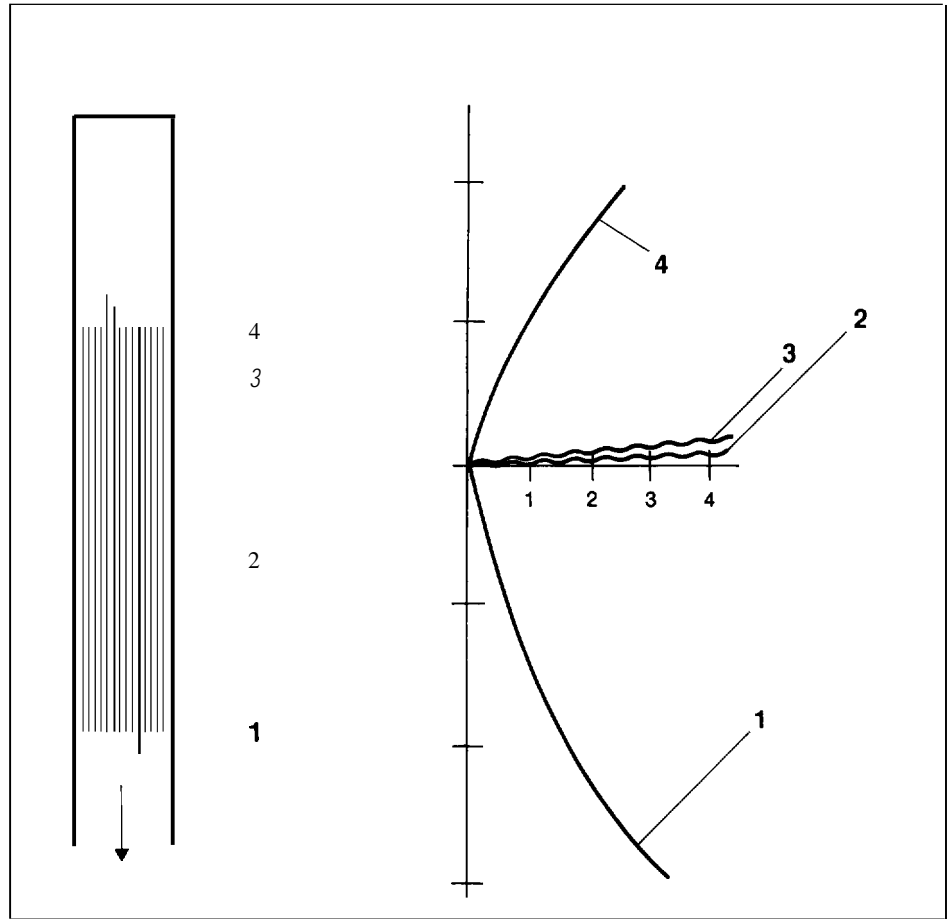


**Fig. 7. The temperature change  $T - T_{initial}$  of thermocouples placed in a stack of plates of a simple acoustic heat pump shows the effect of symmetry breaking. Application of acoustic power to the tube at time zero immediately produces large changes at the two ends (positions 1 and 4) where thermodynamic**

**symmetry is broken geometrically. Much smaller changes occur at the middle of the stack (position 2) and relatively close to the end (position 3) that are a consequence of a weak dynamic symmetry breaking due to viscosity and the nonuniformity of the acoustic pressure and velocity fields.**

adiabatic compression, and no heat flows between the gas and the plate. (Because of losses in a real engine, the maximum temperature gradient that can be produced by a heat pump is somewhat less than  $\nabla T_{crit}$ , and the minimum gradient needed to drive a prime mover is somewhat greater than  $\nabla T_{crit}$ .)

**Thermoacoustic Couple.** The thermoacoustic couple is a simple thermoacoustic device. A calculation of the properties of the thermoacoustic couple demonstrates a good deal of the physics of natural thermoacoustic engines and can be done quantitatively from first principles (see "The Short Stack"). When suitably calibrated, the device can also be used as a probe to measure both acoustically stimulated heat flow and acoustic power.

Typically, such a probe is a single short thin plate of the type used in an acoustic

engine (or a small stack of such plates) that can be moved to various longitudinal positions in an acoustical resonant tube. A speaker at the open end of the tube drives the acoustic oscillations.

The material of the plate has a large thermal conductance so that no *substantial* temperature gradient can build up along its length, ensuring that the couple operates under a low temperature gradient as a heat pump. As the probe is moved to various locations in the standing acoustic wave, it measures a flow of heat generated by its presence by detecting a small temperature drop across its length.

Data taken with such a probe (Fig. 9) fit a simple sine curve whose period is *half* the wavelength of the acoustic standing wave. By noting how the sign of the temperature difference varies with respect to the plate's location in the sound wave, we see that heat always flows in the direction

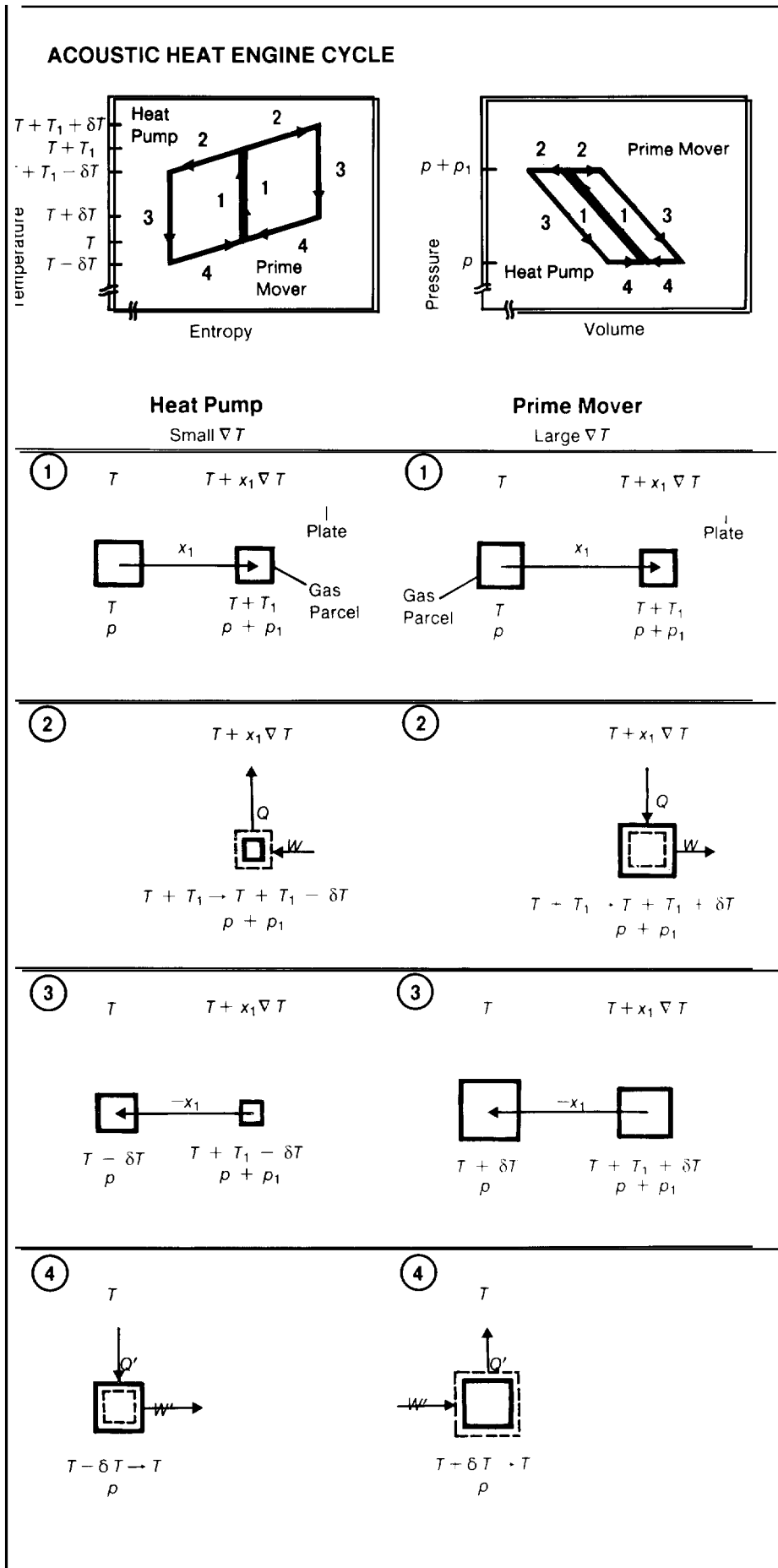
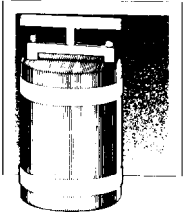


Fig. 8. The thermodynamic cycles (top) of the gas parcels in an acoustic heat engine consist of reversible adiabatic steps and irreversible constant-pressure steps (the acoustic mode is here simplified to articulated rather than sinusoidal motion). This cycle is identical to the Brayton cycle. If we follow a parcel of gas as it moves alongside a fiber glass plate, we see that the prime-mover mode (red) occurs when the temperature rise seen by a gas parcel on the adjacent plate due to displacement of the gas along the gradient ( $x_1 \nabla T$ ) is larger than the temperature rise of the gas due to adiabatic compression heating of the gas ( $T_1$ ). The heat-pump mode (black) occurs under the opposite conditions, that is, when the gradient on the plate is zero or low. In the prime-mover mode, the pressure ( $p + p_1$ ) during the heat-flow expansion step is larger than the pressure ( $p$ ) during the heat-flow compression step, so net work is added to the acoustic vibration. All flows are reversed in the heat-pump mode, and work is absorbed from the acoustic vibration. ◀

of the closest pressure antinode. This effect is expected from the description of the heat pump in Fig. 8 because a parcel of gas moving in the direction of a pressure antinode is compressionally warmed and will transfer heat to the low-gradient plate; a parcel moving toward a pressure node is cooled by expansion and will draw heat from the plate. This explains the surprising results of the half-wave resonator heat pump of Merkli and Thomann (Fig. 5b).

At both the pressure antinodes and the pressure nodes, heat flow in the couple drops to zero. This effect occurs because the pressure and the gas velocity in a resonant acoustic wave are spatially 90 degrees out of phase. Thus, a pressure antinode is also a velocity node, and heat flow drops to zero because there is no displacement of gas. On the other hand, a pressure node has zero heat flow because no compression

*continued on page 16*



# THE SHORT STACK

To calculate thermodynamic efficiency for an acoustic heat engine, we need to know the hydrodynamic heat flow and the work flow. A heuristic derivation of these two quantities and the resulting efficiency for the particular case of a short stack follow. We then briefly discuss the effects of viscosity.

## Heat Flow

Consider a stack of plates in a heat engine whose length is short compared to the acoustic wavelength and to the distance from the stack to the end of the tube. If that length is short enough, we can ignore the change in the longitudinal acoustic velocity magnitude  $u$ , and the change in the dynamic, or acoustic, pressure magnitude  $p$ , with respect to longitudinal distance  $x$  (measured from the end of the acoustically resonant tube). Further, if we ignore the effects of fluid viscosity,  $u$ , does not depend on lateral distance from the plates. Next, we can take the lateral distance between plates to be large compared to the thermal penetration depth  $\delta_x$  (the characteristic length for heat transfer in the fluid during a given cycle of the acoustic wave). Thus, and effects we estimate for a stack of plates will be the same as the a single plate having the same overall perimeter  $\Pi$  (measured transverse to the flow).

The adiabatic temperature change  $T_1$ , accompanying the pressure change  $p_1$ , can be derived from thermodynamics and is

$$T_1 = \frac{T_m \beta}{\rho_m c_p} p_1, \quad (1)$$

where  $T_m$  is the mean absolute temperature,  $\beta$  is the isobaric expansion coefficient,  $\rho_m$  is the mean density, and  $c_p$  is the specific heat at constant pressure.

The change of entropy for a parcel oscillating in the manner depicted in Fig. 8 of the main text is just the lateral heat flow from the second medium divided by  $T_m$  or  $\rho_m c_p \delta T / T_m$  per unit volume, where  $\delta T$  is the change in the fluid temperature due to that heat flow. The volume transport rate for that part of the fluid that is thermodynamically active is  $\Pi \delta_x u_1$ . We thus can estimate the flow of hydrodynamically transported heat  $\dot{Q}$  as the product of these two quantities times  $T_m$ ; that is,

$$\dot{Q} \sim \Pi \delta_x u_1 \rho_m c_p \delta T. \quad (2)$$

Now from Fig. 8 we also see that

$$\delta T = T_1 - x_1 \nabla T = T_1 \left( 1 - \frac{\nabla T}{T_1/x_1} \right), \quad (3)$$

where  $\nabla T$  is the temperature gradient along the plate and  $x_1$  is the fluid displacement. The value of  $\nabla T$  that makes  $\delta T = 0$  is the critical gradient, so

$$\nabla T_{\text{crit}} = \frac{T_1}{x_1}. \quad (4)$$

Combining these equations and defining the temperature gradient ratio parameter as  $\Gamma \equiv \nabla T / \nabla T_{\text{crit}}$  gives an estimate for the hydrodynamic heat flow as

$$\dot{Q} \sim -\Pi \delta_x (T_m \beta) p_1 u_1 (\Gamma - 1). \quad (5)$$

The parameter  $T_m \beta$  is what we call the *heat parameter* of the fluid. The presence of the  $\Pi \delta_x$  factor is obvious because it is the thermodynamically active area in a plane perpendicular to the longitudinal acoustic motion. The formula shows that when  $\Gamma < 1$ , heat flows up the temperature gradient, as for a heat pump; when  $\Gamma = 1$ , there is no heat flow; when  $\Gamma > 1$ , heat flows down the temperature gradient, as for a prime mover.

## Work Flow

Now that we have estimated the heat flow, we need to calculate the work flow, which is given by the work per cycle (the area  $p_1 \delta V$  enclosed by the pressure-volume diagram in Fig. 8 of the main text) times the rate at which that work occurs (the angular acoustic frequency  $\omega$ ). The volumetric change  $\delta V$  that will contribute to the net work is just

$$\frac{\delta V}{V} = \beta \delta T, \quad (6)$$

where  $\delta T$  is the temperature change of Eq. 3.  $V$ , the total volume of gas that is thermodynamically active, is given by

$$V = \Pi \delta_x \Delta x, \quad (7)$$

where  $\Delta x$  is plate length.

We can now simply put these pieces together and, using Eqs. 1, 3, 6, and 7, write down the work flow as

$$\begin{aligned} \dot{W} &\sim p_1 \delta V \omega \\ &\sim \Pi \delta_x \frac{T_m \beta^2}{\rho_m c_p} p_1^2 \omega \Delta x (\Gamma - 1). \end{aligned} \quad (8)$$

From thermodynamics we know that

$$\gamma - 1 = \frac{T_m \beta^2 a^2}{c_p}, \quad (9)$$

where the quantity  $\gamma - 1$  is what we call the *work parameter* of the fluid, and  $a$  is the speed of sound, so we can rewrite the expression for work flow as

$$\dot{W} \sim \Pi \delta_x (\gamma - 1) \frac{p_1^2}{\rho_m a} (\Gamma - 1) \frac{\Delta x}{\lambda}, \quad (10)$$

where  $\lambda = a/\omega$  is the radian length of the acoustic wave.

The formulas for estimating  $\dot{Q}$  and  $\dot{W}$  (Eqs. 5 and 10) have a very similar structure, which is expected since they are closely related thermodynamically. The heat parameter  $T_m \beta$  appears in the formula for  $\dot{Q}$ , and the work parameter  $\gamma - 1$  appears in the formula for  $\dot{W}$ . Both  $\dot{Q}$  and  $\dot{W}$  are quadratic in the acoustic amplitude  $p_1$  or  $u_1$ ; both change sign as  $\Gamma$  passes through unity.

### Efficiency

A quantitative evaluation of  $\dot{W}$  and  $\dot{Q}$  for this case of the short stack but for sinusoidal  $p_1$  and  $u_1$  would give the same results except each formula has a numerical coefficient of 1/4. Thus the efficiency  $\eta$  of a short stack with no viscous or longitudinal conduction losses is

$$\eta = \frac{\dot{W}}{\dot{Q}} = \frac{\gamma - 1}{T_m \beta} \frac{\omega \Delta x p_1}{\rho_m a^2 u_1}. \quad (11)$$

For our standing acoustic wave,  $u_1 = u_0 \sin x/\lambda$  and  $p_1 = \rho_m a u_0 \cos x/\lambda$ , where  $x$  is the distance of the stack from the end of the tube. Then the efficiency can be rewritten simply as

$$\eta = \frac{\gamma - 1}{T_m \beta} \frac{\Delta x}{\lambda \tan x/\lambda}. \quad (12)$$

In the important limit of  $x \ll \lambda$ , the efficiency is simply

$$\eta = \frac{\gamma - 1}{T_m \beta} \frac{\Delta x}{x} \quad (13)$$

Thus, in either case, efficiency depends only on geometry and fluid parameters, just as for the Brayton and Otto cycles discussed in the text. The temperatures  $T_h$  and  $T_c$  do not enter.

As the *actual* temperature gradient approaches the critical temperature gradient  $\nabla T_{\text{crit}}$ , the temperature difference  $\delta T$  approaches zero, so that even at the acoustic angular frequency  $\omega$  the heat transfer rate and the power output approach zero, just what is needed to give the Carnot efficiency in the Brayton and Otto cycles. What happens in this engine? We use Eqs. 1, 4, and 9 and the fact that  $u_1 = x_1 \omega$  to rewrite the efficiency formula (Eq. 11) in general as

$$\eta = \frac{\Delta x \nabla T_{\text{crit}}}{T_m} \quad (14)$$

Because  $\Delta T = \Delta x \nabla T_{\text{crit}}$  when  $\nabla T = \nabla T_{\text{crit}}$ , we have at the critical temperature gradient

$$\eta = \frac{\Delta T}{T_m}. \quad (15)$$

The Carnot efficiency is  $\eta_C = 1 - T_c/T_h$ . But if  $T_c = T_h - \Delta T$ , and if  $\Delta T/T_h$  is small so that  $T_h$  can be replaced by  $T_m$ , we get, with our approximations, the same formula for  $\eta_C$  as Eq. 15. So the acoustic engine approaches Carnot's efficiency as the power output and heat transfer rates approach zero, just like the Otto and Brayton cycles.

### What About Viscosity?

So far we have assumed that the working fluid is inviscid. What if it is not? We know how to do the theory quantitatively for this more general case, but the resulting expressions for  $\dot{Q}$  and  $\dot{W}$  are terribly complicated and opaque. We can simplify

them by assuming that the Prandtl number (the square of the ratio of the viscous penetration depth  $\delta_v$  to the thermal penetration depth  $\delta_x$ ) is small. In that case we obtain

$$\dot{Q} = \frac{1}{4} \Pi \delta_x (T_m \beta) p_1 u_1 (\Gamma - 1) - \frac{1}{4} \Pi \delta_v (T_m \beta) p_1 u_1 \quad (16)$$

$$\dot{W} = \frac{1}{4} \Pi \delta_x (\gamma - 1) \frac{p_1^2}{\rho_m a} \frac{\Delta x}{\lambda} (\Gamma - 1) - \frac{1}{4} \Pi \delta_v \rho_m a u_1^2 \frac{\Delta x}{\lambda}. \quad (17)$$

To lowest order, then, the effect of viscosity on heat flow is just to decrease  $\dot{Q}$  by a term proportional to the viscous penetration depth. This simply means that viscosity prevents a layer of fluid of thickness  $\delta_v$  adjacent to the plate from moving acoustically and contributing to the acoustically stimulated heat transport. Similarly, the work flow is decreased by a term proportional to  $\delta_v$ ; this term is simply the energy lost from the acoustic wave due to viscous drag on the plate.

For simplicity in Eqs. 16 and 17 we have kept our old definition of  $\nabla T_{\text{crit}}$ , even though another effect of viscosity is to make the concept of a critical temperature gradient less well defined. In fact, with viscosity present there is a lower critical gradient below which the engine pumps heat and a higher critical gradient above which the engine is a prime mover. Between these two gradients the engine is in a useless state, using work to pump heat from *hot* to *cold*.

The Prandtl number for helium gas is about 0.67, so that viscous effects are very significant for our gas acoustic engines (and, in fact, Eqs. 16 and 17 are rather poor approximations). On the other hand, the Prandtl number for liquid sodium is about 0.004, so that viscous effects are much smaller. ■

*continued from page 13*

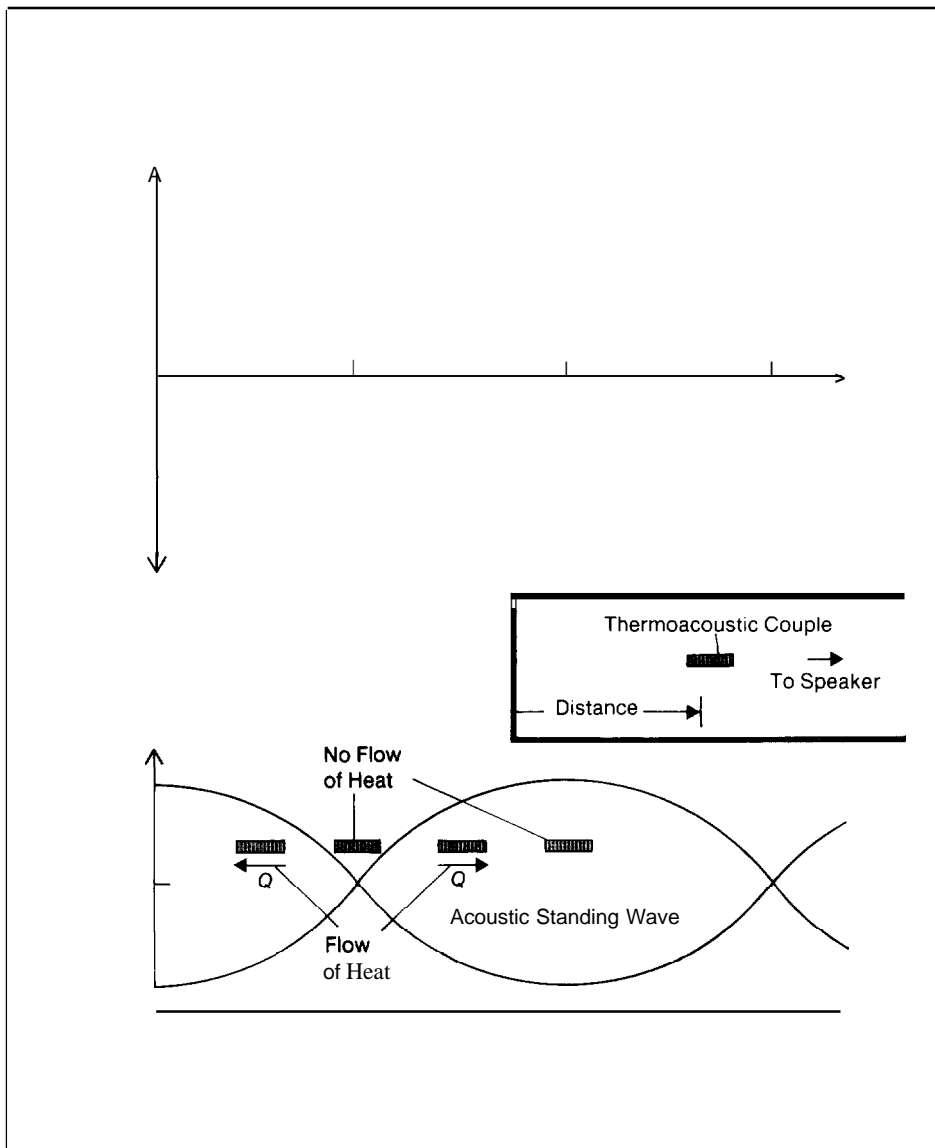
or expansion takes place. In other words, acoustic heat flow depends on both the acoustic pressure and the fluid velocity.

Figure 9 also illustrates the dramatic effect the positioning of a plate in the acoustic wave has on the operation of a natural heat engine. A plate or stack of plates placed completely within a quarter of a wavelength of the end of the tube operates in the manner depicted in Fig. 8. If that same stack is repositioned in the second quarter of a wavelength, the pictorial analysis of Fig. 8 still applies, but the directions of all heat flows and longitudinal temperature gradients are reversed. A stack that extends beyond an adjacent node-antinode pair, however, has heat flows that counter each other, canceling part of the overall transport of heat from one end of the plates to the other,

Also important is the stack's position *within* a given node-antinode pair separated by a quarter of an acoustic wavelength (Fig. 10). For an engine in the heat-pump mode, a stack close to a pressure antinode—say, the end of the tube—can develop steep temperature gradients. Why? In such a region the acoustic pressure change in a parcel of gas is large and thus the rise in temperature from compressional warming is large. This region is also near a velocity node, so displacement of the gas parcel is small. Large temperature changes over small displacements, of course, result in large temperature gradients. (Or one can say that  $\nabla T_{crit}$ , which bounds the region between the heat-pump and prime-mover modes, is large close to a pressure antinode.)

As a plate or stack of plates is moved away from the pressure anti node, the temperature gradient developed becomes smaller. At a quarter of a wavelength, no gradient forms ( $\nabla T_{crit}$  equals zero). This positioning effect is important in the design of a refrigerator, because, together with the length of the plates, it places an upper limit on the maximum temperature drop possible across the stack.

Positioning also affects the losses that



characterize an engine. For example, a stack close to a pressure antinode is close to a velocity node, and viscous losses will be small at that position. However, because temperature gradients are steep there, losses from ordinary diffusive thermal conduction in the plates and working fluid will be increased. The problem of ordinary conduction losses is especially critical for an engine acting as prime mover because such an engine needs a temperature gradient higher than

$\nabla T_{crit}$  to work. Thus, the positioning of the set of plates is a tradeoff between viscous losses, losses from longitudinal conduction, the desired temperature span across the engine, and power output.

**Heat and Work.** We can now better understand the natural acoustic engine by examining what happens near a short plate positioned between a node and an antinode (Fig. 11). If the displacement of a given parcel of gas is small with respect to

**Fig. 9. The temperature difference  $\Delta T$  measured across a thermoacoustic couple as a function of the plate's position in the acoustic standing wave. Note that heat flows toward the closest pressure antinode, making that end of the couple hottest. However, at both the pressure antinodes and nodes there is no flow of heat ( $\Delta T = 0$ ). These data were obtained for an acoustic wavelength of approximately 80 cm. ◀**

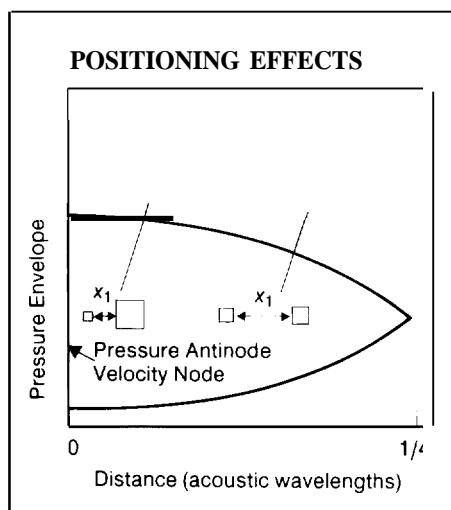


**Fig. 10. Close to a pressure antinode a typical parcel of gas experiences large changes in pressure  $p$ , and thus large changes in temperature  $T$ , due to compressional heating. At the same time, displacement  $x_1$  of the parcel is small, so that  $\nabla T_{\text{crit}} = T_1/x_1$  is large; in fact, since  $x_1$  is proportional to the distance  $x$  from the pressure antinode,  $\nabla T_{\text{crit}} \propto x^{-1}$ . In the heat pump mode, the maximum temperature gradient that can be developed is equal to  $\nabla T_{\text{crit}}$  (since heat flow between gas parcel and plate stops when that gradient is reached), which means that close to a pressure antinode we can expect large temperature gradients. Further from the pressure antinode, pressure and temperature changes become smaller whereas displacements become larger, so the maximum temperature gradient that can be developed is smaller. A**

the length of the plate, there will be an entire train of adjacent gas parcels, each confined in its cyclic motion to a short region of length  $x_1$  and each reaching the same extreme position as that occupied by an adjacent parcel half a cycle earlier. What is the net result of all these individual cycles on the flow of heat and work?

If the motion of the parcels is sinusoidal, only those about a thermal penetration depth\* from the nearest plate are thermoacoustically effective. Parcels close to a plate transfer heat to and from the plate in a locally isothermal and reversible manner, just like the fluid in the regenerator of a Stirling engine. Parcels far away have no thermal contact and are simply compressed and expanded adiabatically and reversibly by the sound wave. However, parcels that are at about a thermal penetration depth from a plate have good enough thermal contact to exchange some heat with the plate but, at the same time, are in poor enough contact to produce a time lag between motion and heat transfer.

During the first part of the cycle for the heat-pump mode, the individual parcels will each move a distance  $x_1$  toward the pressure antinode and deposit an amount of heat  $Q$  at that position on the plate. During the second half of the cycle, each parcel moves back to its starting position and picks up the same amount of heat  $Q$  from the plate. But this heat was deposited there a half cycle earlier by an adjacent parcel of gas. In effect, an amount of heat  $Q$  is merely passed along the plate from one parcel of gas to the next in the direction of the pressure antinode. Thus, as in the Stirling engine, the second thermodynamic medium is used for the temporary storage of heat.

At the ends of the plates, the thermody-

\*The thermal penetration depth  $\delta_\kappa$  is the characteristic length describing heat diffusion through the gas during one period of the acoustic cycle. Mathematically,  $\delta_\kappa = \sqrt{\kappa/\pi f}$ , where  $\kappa$  is the thermal diffusivity of the gas and  $f$  is the frequency of the sound.

amic symmetry is broken. Parcels of gas that move farther from the end of the plate than a thermal penetration depth idle through part of their cycle without accepting or rejecting heat. For example, if a parcel of gas at the end closest to the antinode is in equilibrium with the plate on one half of the cycle but then moves out of the range of thermal interaction, it has nowhere to deposit the heat resulting from its adiabatic warming. As this parcel completes its cycle, it cools adiabatically back to the temperature of the plate. The heat transferred to the plate from the next adjacent parcel down the line is uncompensated, so there is a net heat transfer to the plate on that end, and the temperature of the plate increases there. In similar fashion, heat drawn from the end closest to the node is not replaced, and that end cools. We can take advantage of the net effect—a flow of heat from one end to the other—by bringing the ends of the plates into contact with heat exchangers.

During each cycle an individual parcel of gas transports heat  $Q$  across only a small temperature interval along the plate that is comparable to the adiabatic temperature change  $T_c$ . However, because there are many parcels in series, the heat  $Q$  is shuttled down the stack, thereby traversing the temperature interval  $T_h - T_c$ , which can be much larger than  $T_c$ . Within the limits of a quarter of a wavelength, the flow of heat is not a strong function of plate length (in fact, for a stack much shorter than a quarter of a wavelength, heat flow does not depend on plate length at all).

If, on the other hand, we examine this train of gas parcels with respect to the flow of work, we realize that *each* parcel has a net effect. For example, a parcel of gas near the plates in an engine operating in the heat-pump mode absorbs net work because its expansion is at a lower pressure than the corresponding compression. But since the same is true for every parcel in the train, the total work done on the gas is roughly proportional to plate length (for a very short stack, work flow is proportional to plate length).

**Efficiency.** A calculation of heat and work flows for an acoustic heat engine with a short stack close to the end of the resonator tube and no viscous losses (see "The Short Stack") yields a limiting efficiency given by

$$\eta = \frac{\gamma - 1}{T_m \beta} \frac{\Delta x}{x} \quad (3)$$

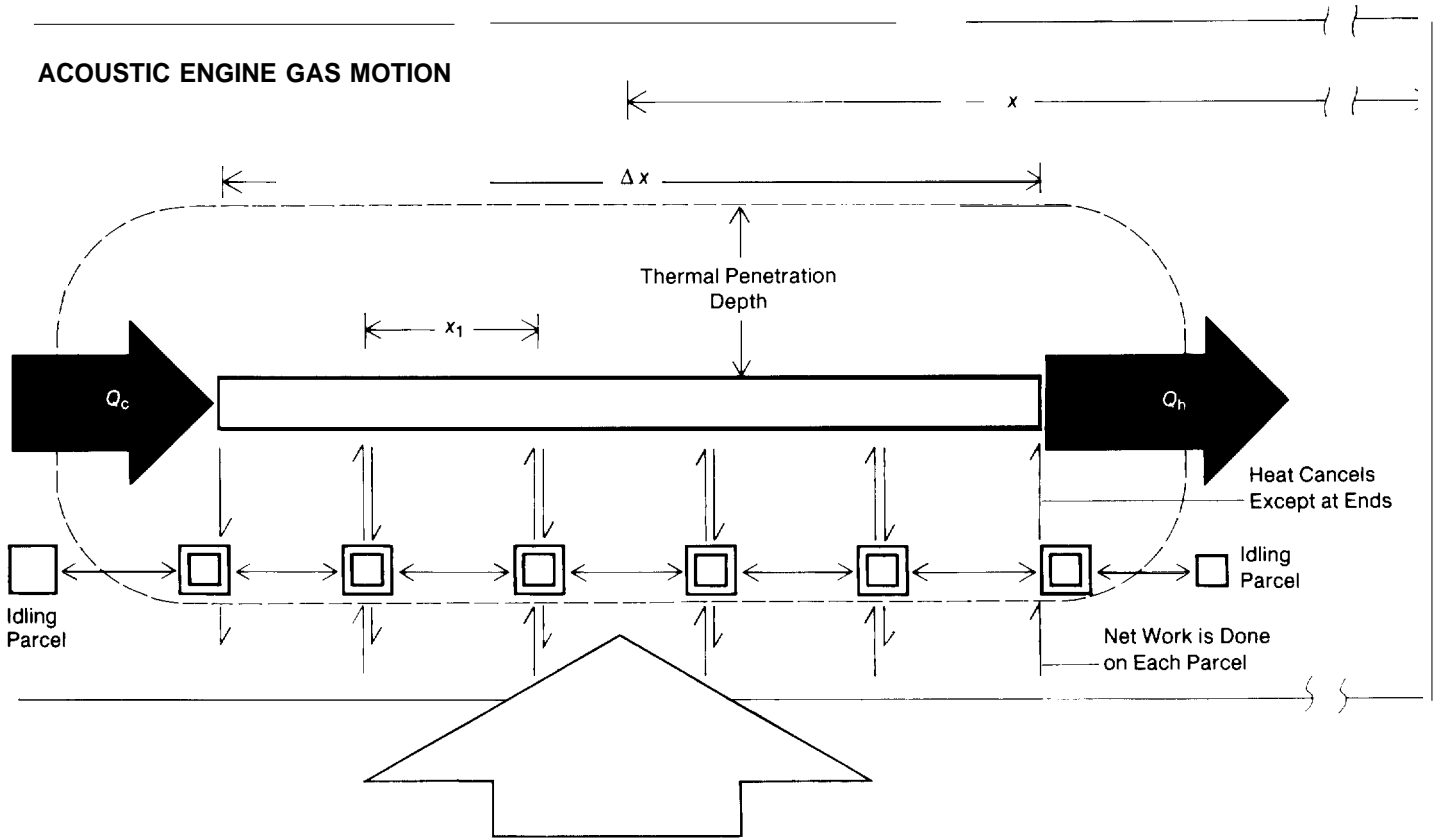
where  $T_m$  is the mean absolute temperature of the plates,  $\beta$  is the isobaric expansion coefficient,  $\Delta x$  is the plate length, and  $x$  is the distance of the plates from the

pressure antinode (usually the end of the tube). This efficiency depends on properties of the working fluid (the *work parameter*  $\gamma - 1$  and the *heat parameter*  $T_m \beta$ ) and on the geometry of the engine ( $\Delta x/x$ ), as in the Otto and Brayton cycles, rather than on the hot and cold temperatures, as in the Carnot and Stirling cycles.

It can also be shown that when the temperature gradient along the plates equals  $\nabla T_{crit}$ , Eq. 3 reduces to the Carnot efficiency. This result is expected because, for such a gradient, rates of heat transfer approach zero, all processes approach re-

versibility, and no entropy is generated during the cycle. Once again, however, the approach to maximum efficiency means an approach to zero power.

**A Natural Magnetic Engine.** To help emphasize the generality of natural engines, we now discuss a hypothetical natural *magnetic* engine. The acoustic engine uses a fluid as its primary medium; our postulated natural magnetic engine uses a solid magnetic material. Further, the operation of the acoustic engine is based on the adiabatic change of temperature with pressure in a fluid, whereas the mag-



▲ Fig. 11. An acoustic heat engine can be thought to have a long train of adjacent gas parcels, all about a thermal penetration depth from the plate, that draw heat from the plate at one extreme of their

oscillatory motion and deposit heat at the other extreme. However, idling parcels at both ends oscillate without removing or depositing heat. Adjacent heat flows cancel except at the ends;

the net result is that an amount of heat  $Q$  is passed from one end of the plate to the other. Adjacent work contributions do not cancel, so that each parcel of gas contributes to the total work.



Tom Hofer attaching the resonator of the cryocooler to the housing of the cooler's driver and hot heat exchanger.

netic engine is based on the *adiabatic change of temperature with magnetization*.

The primary medium of our hypothetical apparatus (Fig. 12) consists of a stack of magnetic disks.\* Each disk has a high internal thermal conductance, but each is also thermally insulated from the others so that a large temperature gradient can be sustained in the longitudinal direction.

The collection of disks is placed in a tube whose walls constitute the second medium. Like the first medium, the second has a high lateral thermal conductance, a large heat capacity, and a low, longitudinal thermal conductance. Thus, it, too, can sustain a large temperature

gradient parallel to the direction of relative motion between the two media.

The device is positioned between the poles of a permanent magnet in such a way that the disks of the primary medium are in the nonuniform fringing field at the side. The disks are linked mechanically to an external mechanism so that they can be moved in a reciprocating fashion. A gas fills the small annular space around the magnetic disks, providing lateral thermal contact with the second medium, but this contact is poor enough to create the necessary phasing for the engine. There is also some means for heat exchange with external reservoirs at each end of the second medium.

\*We simplify our discussion by assuming the magnetic material is an ideal Curie-law paramagnet, for which the magnetization  $m$  is given by  $m = \lambda H/T$  and the entropy  $S$  is given by  $S = S_0 - (\lambda/2) H^2/T^2$ , where  $H$  is magnetic field,  $T$  is temperature, and  $\lambda$  and  $S_0$  are constants. Thus, for adiabatic processes  $m$  is constant; for constant-field processes  $m$  decreases as  $T$  increases.

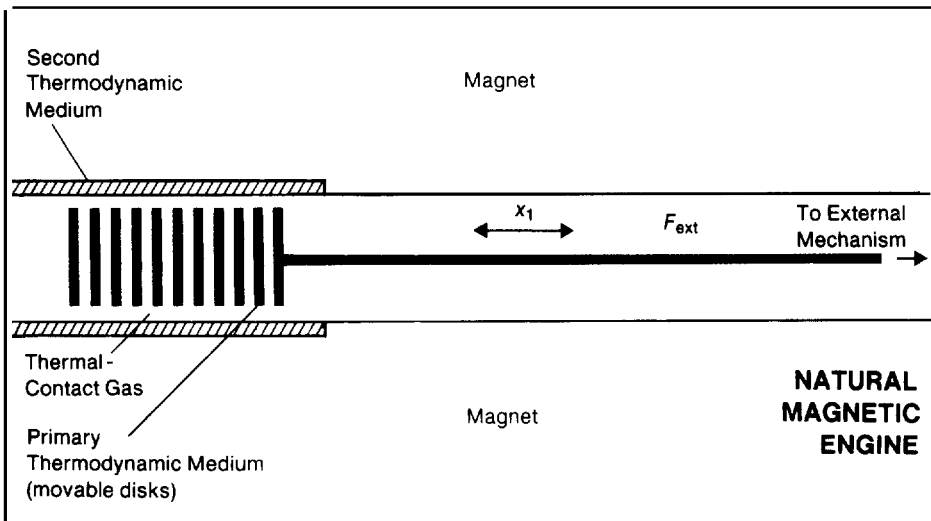


Fig. 12. A hypothetical natural magnetic engine in which the primary medium consists of magnetic disks placed in the fringing field at the side of a permanent magnet. This placement allows an external mechanism to displace the disks in a reciprocating fashion in the presence of a magnetic field gradient. A gas

surrounding the disks makes thermal contact with the second medium (the walls of the tube), but conductivity of the gas is poor enough to create the necessary phasing for the engine. In both media, thermal conductance is poor longitudinally so that large temperature gradients can be supported. A

If we follow an element of the first thermodynamic medium in a magnetic engine through an articulated cycle (Fig. 13), we see that the various steps are analogous to those of an acoustic heat engine. For example, in the first step of a heat-pump cycle, the element is metered quickly and adiabatically to a region of higher magnetic field. As a result, its temperature rises. (Temperature changes of a few degrees per tesla are typical for ferromagnetic and strongly paramagnetic materials.) In the second step, the element thermally relaxes, its temperature adjusting to that of the adjacent region in the second medium, which, in the heat-pump mode, means that heat flows from the first medium to the second. As the element cools, its magnetization increases. The third step is motion back to a region of lower field; the fourth is another thermal relaxation. As in the case of acoustic engines, the phasing between motion and heat transfer is a result of the natural time delay caused by diffusion of heat between the two media.

### Some Applications of Natural Engines

What happens now if these ideals of natural engines are put into practice? What are the clanking, hissing realities of real natural engines?

**Cryocooler.** As part of his Ph.D. thesis, Tom Hofler designed and built a device called the cryocooler (Fig. 14) in which the numerical aspects of the design were based on the general thermoacoustic theory of Rott for ideal gases.

The cryocooler is an acoustic cooling device with a number of important features. Perhaps the most important is the fact that the acoustic resonance is driven from the *hot* end of the stack. All the early cooling engines were arranged with the stack near the closed end of the acoustic resonator tube and with the acoustic driver at the opposite end. Very large temperature differences (about 100 centigrade degrees) could be easily induced across the entire stack this way, but the cold end was seldom less than 20 degrees below ambient temperature. The problem was that the driver (at ambient temperature) and the cold end of the stack maintained moderately good thermal contact with one another by means of *acoustic streaming*. This phenomenon is a second-order, steady circulatory flow of the working gas that is superimposed on the oscillatory motion. The effect of the acoustic streaming was to use up a substantial amount of the refrigeration available at the cold end of the stack trying to cool down the driver.

Now while it is necessary for work to flow into the stack to pump heat, we realized that it is of no real importance whether that flow occurs at the cold or the hot end. Putting the driver at the hot, or closed end, means that none of the available refrigeration is used to cool the driver. Thus, with the "closed" end replaced by a movable piston acting at high dynamic pressure and low displacement, performance is improved.

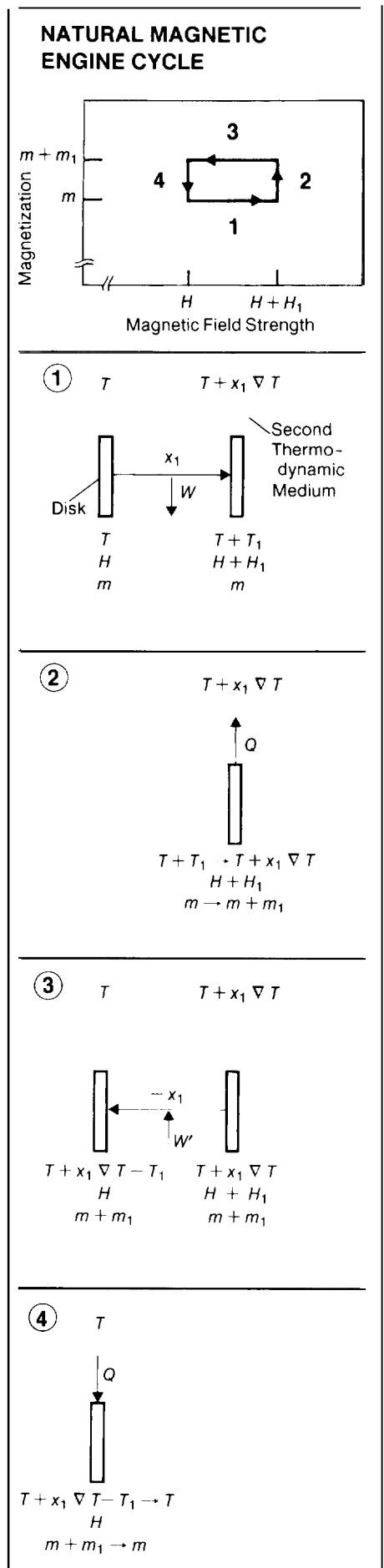
The stack with its heat exchangers was placed rather close to the driver piston, that is, rather close to a pressure anti node. As noted earlier (see Fig. 10). such a region has the high critical temperature gradient needed for a heat pump. Of course, some separation between driver and stack is necessary because acoustically stimulated heat transfer is proportional to the dis-

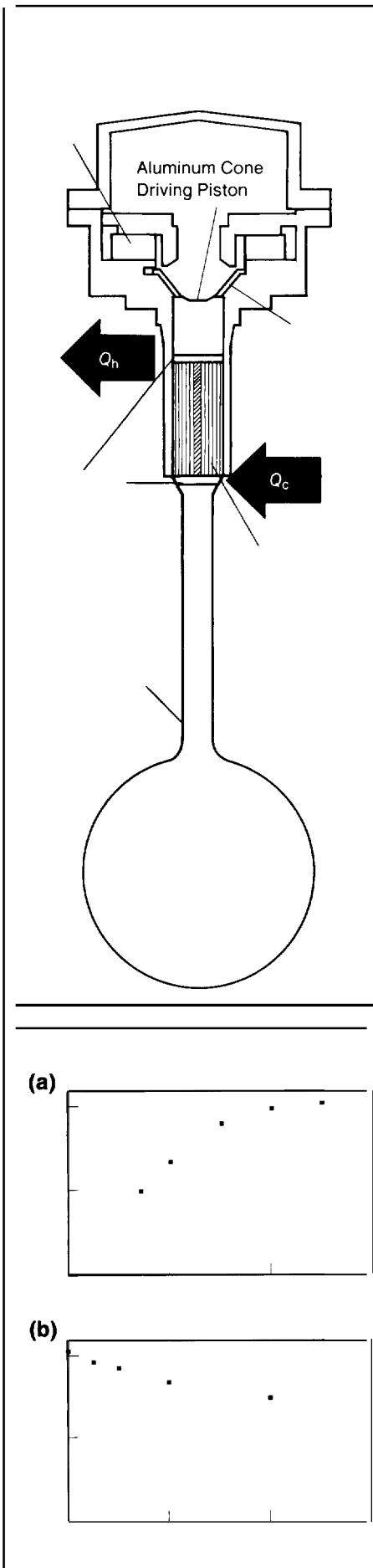
placements of the parcels of gas.

Such a configuration means the remainder of the resonator tube can beat the cold temperature, allowing it to be just a thermally insulated straight tube roughly half an acoustic wavelength long. However, losses due to the dynamical effects of viscosity and thermal conduction along the walls of the resonator reduce the externally available refrigeration. Roughly half this loss could be eliminated by using a quarter-wavelength resonator with one end open, but an open end eliminates the use, say, of several atmospheres of helium as the working fluid and revives the original heat load problem of acoustic streaming—here between the driver and the atmosphere. Moreover, an open end is downright noisy, radiating useful work out into the room.

The simple solution is to replace approximately half the half-wavelength resonator with a closed container of substantial volume. Dynamic pressure will be small in a region of large volume. making the losses correspondingly small. The res-

**Fig. 13. The cycle shown here for the heat-pump mode of a hypothetical natural magnetic engine is analogous to the cycle for the heat-pump mode of the acoustic heat engine (Fig. 8) with magnetic field strength  $H$  taking the role of pressure and magnetization  $m$  taking the role of volume. Thus, the cycle consists of reversible adiabatic steps and irreversible constant-field steps. For an ideal Curie-law paramagnet,  $m \propto H/T$ . Thus, in the first step, when the disk moves adiabatically to a region of higher magnetic field, magnetization remains constant and temperature rises with increasing  $H$ . In the second step, heat flows to the lower temperature of the second medium, causing the disk to cool at constant  $H$  and the magnetization to increase. The net result of all four steps is the transport of heat up the gradient as a result of the work (which will equal  $mH_1$ ) needed to move the disk through its cycle. ►**





onator below the stack was modified further by *decreasing* the diameter of the confining tube and shortening its length. This last modification, at first sight, would appear to be of negative value as one would expect viscous losses to go up; but, for small decreases in neck diameter, dynamic thermal-conduction losses go down

**Fig. 14.** The driver in the acoustic cryocooler is an ultralight aluminum cone attached to the voice coil of a commercial loudspeaker. The second thermodynamic medium, rather than being a set of parallel plates, consists of a sheet of Kapton rolled about a vertical rod and spaced with 15-roil nylon fishing line aligned vertically. Copper heat exchangers are attached at both ends. The form of the bulb and neck, including the constriction, were chosen to reduce viscous and thermal losses by reducing surface area. The device is drawn to scale and is about 50 cm long. ◀

**Fig. 15.** Experimental data for the cryocooler of Fig. 14, obtained with a mean helium pressure of about 10 bars and acoustic frequencies in the range of 540 to 590 Hz. For thermal isolation the engine was placed in an evacuated vessel and surrounded by superinsulation. The frequency was adjusted electronically so the dynamic pressure and velocity were always in phase at the driver. Part (a) shows how the temperature difference between the hot heat exchanger at approximately 26°C and the cold heat exchanger increases with relative dynamic pressure amplitude (the ratio of the acoustic pressure amplitude  $p_1$  at the pressure antinode to the mean pressure  $p$ ). No heat load was applied to the cold heat exchanger. Part (b) shows how, for a relative dynamic pressure amplitude of 0.03, the temperature difference gradually drops with increasing refrigeration load at the cold heat exchanger. ◀

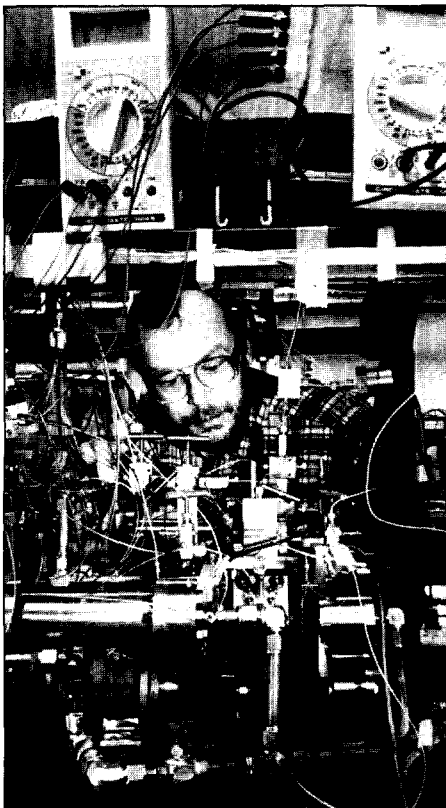
faster than viscous losses go up, and there is a net decrease in the overall losses. These surprising qualities explain the general shape and configuration of the cryocooler.

Performance is rather good (Fig. 15). As the relative dynamic pressure amplitude increases, the temperature difference that can be pumped up for zero external heat load increases, eventually topping out at about  $-100^\circ\text{C}$  when the acoustic pressure amplitude is about 2 or 3 per cent of the mean pressure. At that point, the cryocooler can handle a significant refrigeration load and still maintain a rather low temperature. This type of refrigeration capability is very suitable for cooling instruments and sensors.

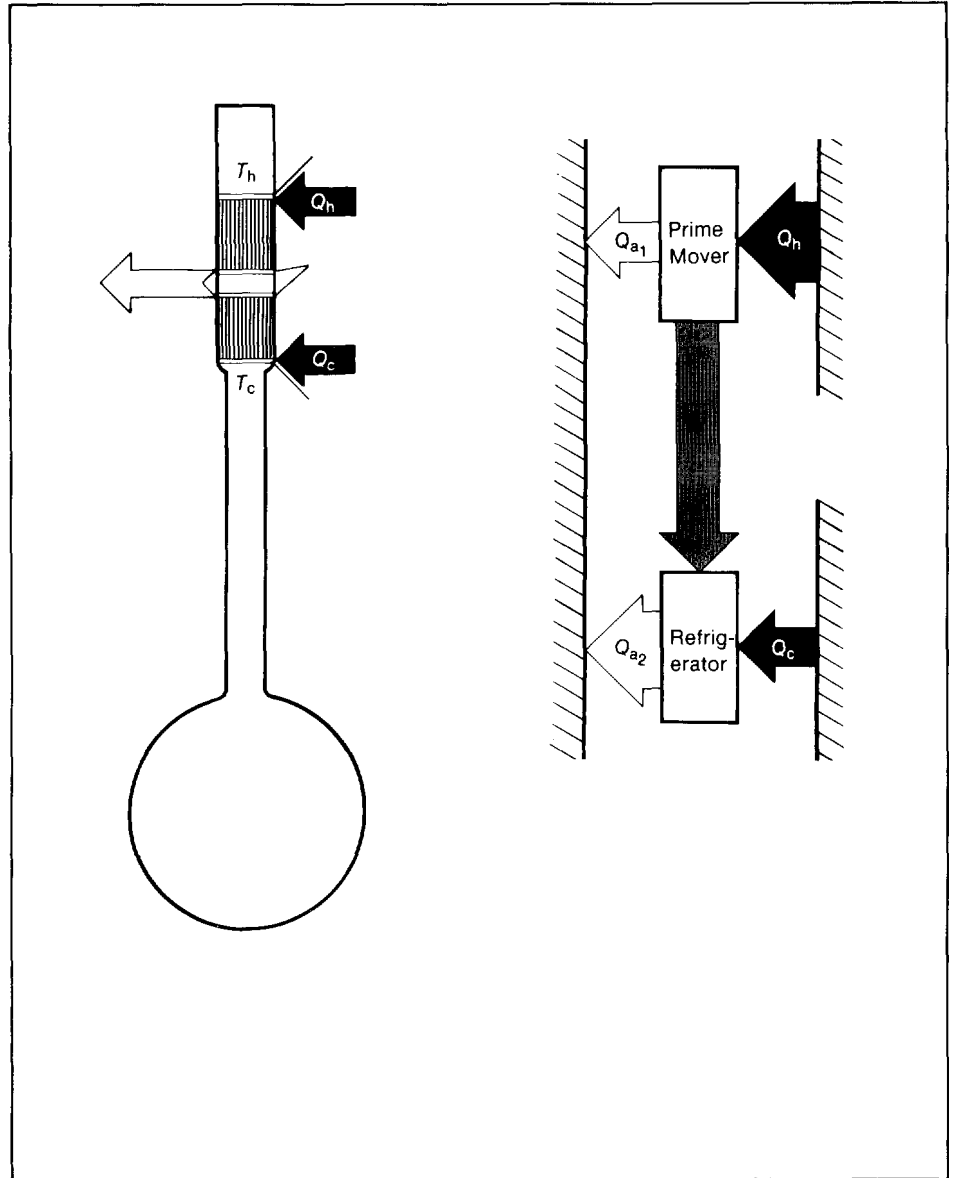
**A Heat-Driven Acoustic Cooler.** Natural acoustic engines are functionally reversible: they can be either prime movers that use heat to produce sound or heat pumps that use sound to refrigerate. Why not combine these two functions in one device and use heat to cool? Such an engine would have heat flow through the walls but no external flow of work.

A key problem in the design of a heat-driven acoustic cooler is where to position the two sets of plates—one set acting as prime mover, the other acting as refrigerator. Ideally, the refrigerator plates should be positioned as they are in the cryocooler, that is, close to the end of the tube where the velocity of the gas and the viscous losses are low but  $\nabla T_{\text{crit}}$  is high. Although it would also be good to keep viscous losses low for the prime-mover plates, it is more important to have these plates near a velocity antinode where  $\nabla T_{\text{crit}}$  is small enough for the stack to develop adequate power. These considerations imply that the refrigerator stack needs to be closer to the end of the tube than the prime-mover stack. However, such a configuration would put the hottest region (the hot end of the prime mover) next to the coldest region (the cold end of the refrigerator), creating a difficult thermal-design problem.

Fig. 16. The upper set of plates in this cooler is a prime mover that draws heat from a heater (at about  $T_h = 390^\circ\text{C}$ ) and rejects waste heat to cooling coils (at  $T_c = 23^\circ\text{C}$  or room temperature), generating acoustic work. The lower engine uses that work to reject heat to the cooling coils (at  $T_c$ ) and to draw heat from an even lower temperature ( $T_c = 0^\circ\text{C}$  or the ice point). The acoustic tube is about half a meter in length, terminates in a 2-liter bulb, and contains helium at a pressure of 3 bars that resonates at a frequency of 585 Hz. Both sets of plates are made of 10-mil (0.025 cm) stainless steel, and the spacing between plates in both sets is 0.08 cm. The hot heat exchanger is made of nickel strips; the ambient and cold heat exchangers of copper. ➤



Bob Oziemski adjusting the flow of the working fluid in the liquid propylene Stirling engine. A



To avoid large heat inputs to the cooler, the positions of the two stacks can be reversed and the various temperatures arranged in decreasing order along the tube. What now becomes paramount is for conditions to be such that the prime mover is able to adequately drive the cooler. Amplification of acoustic fluctuations occurs only above a critical value of  $\Gamma$  ( $\equiv \nabla T / \nabla T_{\text{crit}}$ ). One way to increase  $\Gamma$  is to shorten the prime-mover stack but keep the temperature difference across the stack

constant, thus increasing  $\nabla T$ . Unfortunately, this type of change increases the heat loss due to conduction down the stack.

Another way to increase  $\Gamma$  is to lower  $\nabla T_{\text{crit}}$  by moving the prime-mover stack away from the pressure antinode at the end of the tube. Because of the intervening prime-mover stack, the refrigerator stack is *already* much farther from the pressure antinode than in the cryocooler, and additional movement of the prime-mover

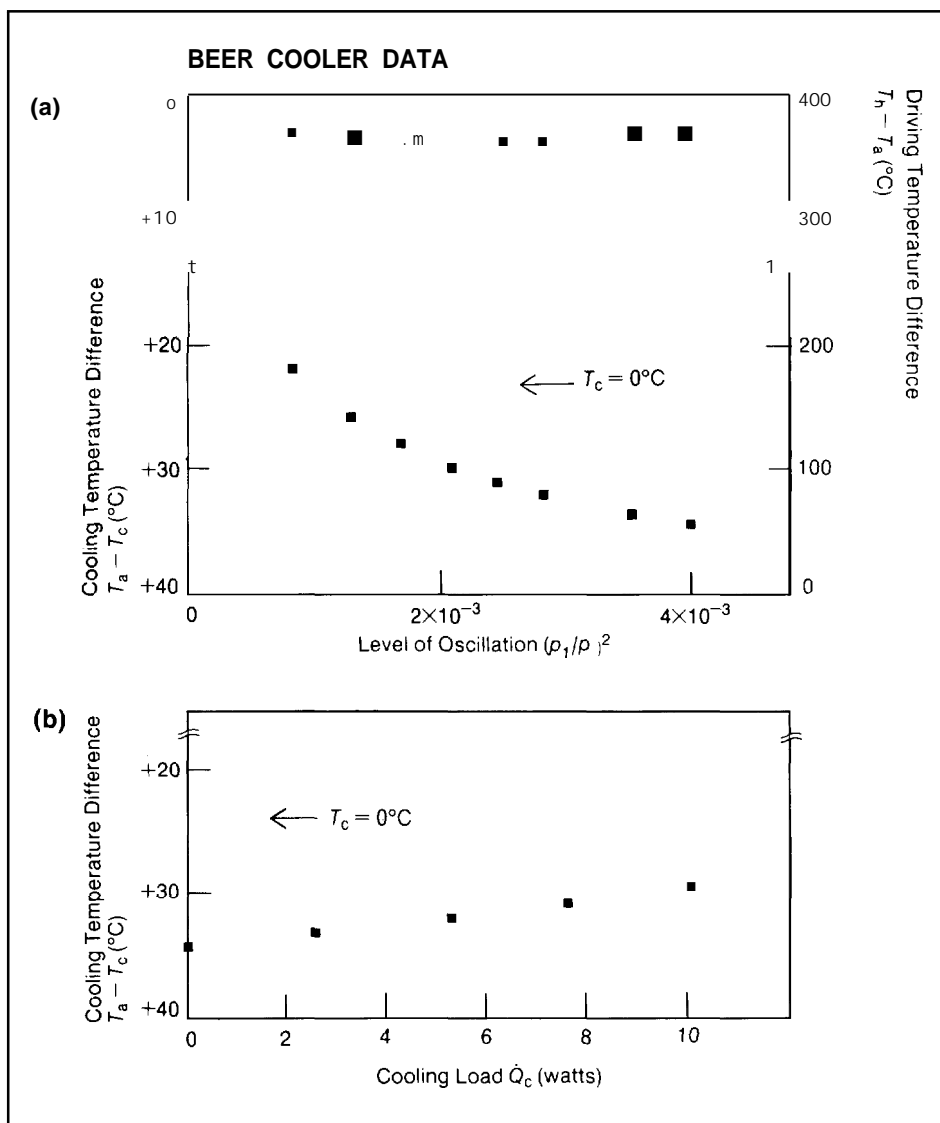


Fig. 17. For these measurements on the beer cooler, the refrigerator stack and the resonator were located in an evacuated space for thermal insulation. Part (a) shows how the cooling temperature difference (black) across the refrigerator stack and the driving temperature difference (red) across the prime-mover stack vary with the level of oscillation (here given by the square of the relative dynamic pressure amplitude) when no external refrigerator load is placed on the cooler. The level of oscillation is determined by the rate at which heat is supplied and removed across the prime-mover stack, but, as can be seen, this results in little change in the driving temperature difference. At the same time, the cold temperature drops gradually below the freezing point of water. (b) For a level of oscillation of about  $4 \times 10^{-3}$  (that is,  $p_1$  is about 0.19 bar), we see that the beer cooler can handle a small heat load of 10 watts and still remain below freezing. ◀

refrigerator stack, thus reducing viscous and acoustic-streaming losses.

In our model engine the plate material in the stacks (stainless steel) and the spacing of the plates were dictated by ease of fabrication as much as by anything else. The refrigerator assembly was placed in an evacuated container but not otherwise thermally insulated. The working fluid was helium, whose pressure was chosen experimentally to minimize the cold temperature. A major problem, yet to be satisfactorily solved, was efficient exchange of heat at the heat exchangers—especially the hot exchanger made of nickel.

In spite of the engine's compromises, it still sings along, performing rather well (Fig. 17). As the heat supplied to the hot end of the prime mover is increased, the level of oscillation increases—the largest peak-to-peak dynamic pressure amplitude measured at the ambient exchangers exceeding a tenth of the mean pressure. In agreement with our understanding, the temperature drop across the prime-mover

stack pushes the refrigerator stack even more from its optimum position. Once again, changing an idea into a practical heat engine entails a set of compromises.

A schematic of an operational heat-driven cooler in which the prime-mover stack is between the end of the tube and the refrigerator stack is shown in Fig. 16. Because of the above considerations—especially those related to  $\nabla T_{\text{crit}}$ —the refrigerator stack in this device cannot be expected to cool much below ambient temperature. Although unable to

produce cryogenic temperatures, the cooler ought to be able to produce temperatures low enough to cool a can of beer. For this reason we have affectionately dubbed the engine the "beer cooler."

As in the case of the cryocooler, the rather complex design was carried out numerically, and many of the features important to the cryocooler apply to the beer cooler. For example, the resonator is similar to the resonator in the cryocooler, and the driver is on the "hot" side of the

stack does not change much as the dynamic pressure amplitude increases; the small changes seen in the data result from the diffusive flow of heat across the gaps of gas and through the heat exchangers from the heat source to the ambient heat exchanger. Figure 17b shows that the beer cooler can manage a 10-watt cooling load while keeping  $T_c$  5 centigrade degrees below the freezing point of water—a rather encouraging result for the first laboratory model.

A number of issues concerning the practical use of this engine concept and of the cryocooler remain to be resolved. It is likely that the most important is the matter of heat exchange. This problem, as we've mentioned, has always been a key one in the development of heat engines—classical or otherwise.

**The Liquid Sodium Acoustic Engine.**

As man moves from Earth into space, so does his need for reliable power. However, differences in the requirements and in the operating environment in space may prompt radical changes in the engines that provide such power. An idea stimulated by such differences is the liquid sodium acoustic engine, which not only is a natural, rather than a conventional, engine but uses a liquid instead of a gas as its working fluid.

The concept of using a liquid can be traced to a 1931 paper by J. F. J. Malone in which he pointed out that certain liquids have important thermodynamic qualities that make them suitable for use in heat engines. Although concerned about its chemical reactivity, Malone knew that liquid sodium was one of these “good liquids,” but materials technology was then inadequate for him to consider its use.

Today's materials technology suggests revival of these ideas, and we had been working on the liquid propylene Stirling engine (see “The Liquid Propylene Engine”) as a modern example of an innovative but more conventional engine that uses liquids. Thus, when we learned

from then Associate Director Kaye Lathrop of the need in space for a reliable, moderately efficient electrical generator, it was not difficult for us to propose a natural acoustic engine based on liquid sodium. Especially ideal for this application is the high “cold” temperature (at least 400 kelvins) of the liquid sodium engine. This fact is important because the cold sink for any heat engine in space must ultimately be a black-body radiator whose size would be proportional to  $T_c^{-4}$

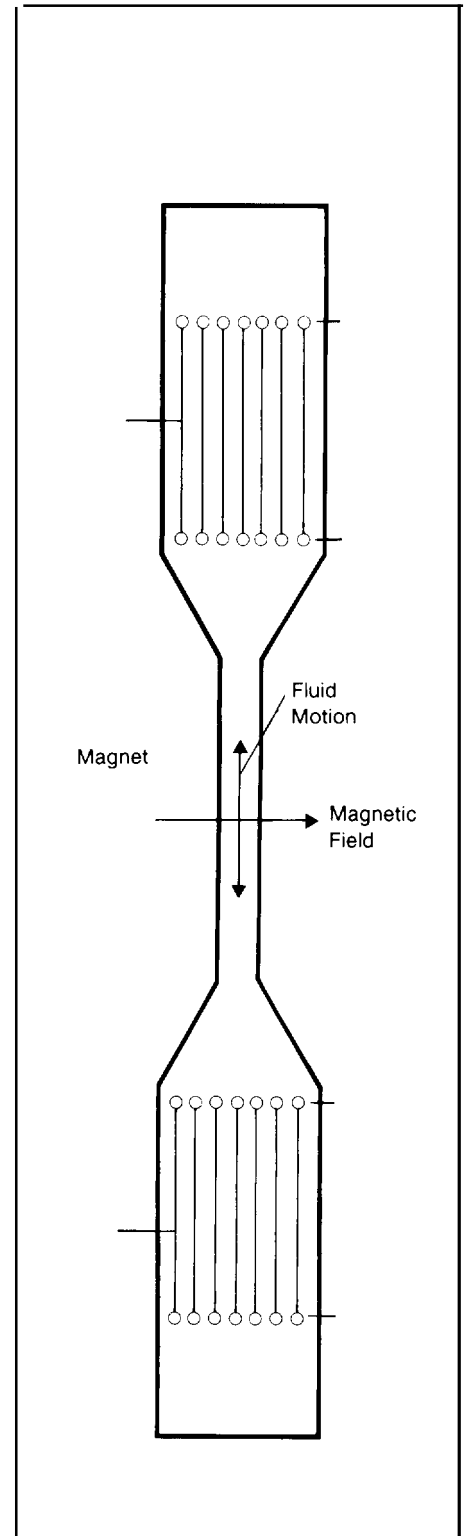
Liquid sodium has many potential advantages as a working substance in a natural engine. The heat and work parameters are acceptably large. For example, at 700°C, which is roughly in the middle of the temperature range of a possible high-power engine, liquid sodium has a very high expansion coefficient and a large ratio of specific heats so that  $T\beta = 0.28$  and  $\gamma - 1 = 0.43$  (compared to a monatomic gas such as helium, for which  $T\beta = 1$  and  $\gamma - 1 = 2/3$ ).

For a given Mach number,\* the power density in the stack is proportional to  $\rho a^3$ , where  $\rho$  is the density of the working fluid and  $a$  is the speed of sound. The density of liquid sodium is about 500 times greater than that of helium at the pressures used in our gas acoustic engines, and the speed of sound is more than a factor of 2 greater. Thus, the power density for a liquid sodium acoustic engine should be more than 10<sup>7</sup> times greater than for a helium acoustic engine, a definite advantage.

This dramatic increase is not without its drawbacks, however. The heat capacity per unit area for the sodium within a thermal penetration depth of the second

\*The Mach number is the ratio of the fluid speed to the speed of sound in the fluid.

**Fig. 18. The temperature drop applied across both stacks of molybdenum plates causes the liquid sodium in this proposed engine to oscillate back and forth between the poles of the magnet. A magnetohydrodynamic effect is used to convert acoustic to electric energy. ➤**





**Chris Espinoza welding heat exchange manifolds onto the resonator tube of the liquid sodium natural heat engine.**

medium is so large that the usual assumption of infinite heat capacity of the second medium is not valid. As a consequence, the power density drops. Moreover, the acoustic impedance  $pa$  of the sodium is relatively high—roughly equal to that of solids—which means that in a sodium engine motion of the stack and container can be expected to send heavy vibrations throughout the entire engine (unlike the beer cooler, for example, in which a peak-to-peak dynamic pressure oscillation of 10 per cent of the mean pressure produces only a pleasantly audible tone in the room). To counter this effect, stiff, high-density materials like molybdenum or tungsten need to be used in the stack, and the walls of the resonator need to be made of heavy stainless steel. Even with such strong walls, high Mach numbers cannot be achieved because the high acoustic pressures would burst the resonator.

Liquid sodium has other very desirable features. For example, its Prandtl number, which can be thought of as the square of the ratio of the viscous penetration depth to the thermal penetration depth, is ex-

tremely low (about 0.004 for sodium at 700°C compared to 0.667 for helium gas). The reason for such a low Prandtl number is that liquid sodium is a metal. As a result, its kinematic viscosity, is rather normal for a liquid, but, owing to electronic contributions to the conduction of heat, its thermal diffusivity is high. The consequences are important. In helium, viscous shear extends into the gas from a boundary about as far as the temperature gradients that drive the flow of heat. This shear drains energy, decreasing efficiency and making it difficult for a gaseous heat engine to work. The low Prandtl number of liquid sodium means that heat can be transported between working fluid and the plates for a volume fifteen times larger than the volume being affected by viscosity, and viscous losses are correspondingly small. Again, however, a price must be paid: diffusive heat conduction in the sodium down the stack increases.

The fact that liquid sodium is a metal has yet another important consequence. Electrical current can be generated from the sound via magnetohydrodynamic coupling. Such coupling means electric power can be produced from heat without using moving parts (ignoring the non-negligible motion of the vessel containing the sodium!). This feature, of course, is one of the main reasons for the expected re-

liability of the engine. Figure 18 is a schematic of a possible liquid sodium prime mover that uses a half-wavelength resonant tube, two driving stacks (one on each side of the magnet), and magnetohydrodynamic power coupling.

To design a model liquid sodium engine, we constructed a thermoacoustic theory for liquids and then evaluated it numerically. The calculated characteristics of a reasonably designed engine are given in Table 1. Note that the dynamic pressure almost equals the mean pressure of the sodium and that efficiency is calculated to be about 18 per cent (31 per cent of the Carnot efficiency).

A complete engine has not yet been built, but work (supported by the Division of Advanced Energy Projects in DOE/BES) has been done separately on the magnetohydrodynamics and the thermoacoustics. In both cases preliminary results are encouraging, though technical problems remain.

First, a magnetohydrodynamic converter was built that consisted essentially of a liquid sodium acoustic resonator with a central rectangular channel for guiding the sodium in the transverse direction between the poles of a magnet. Electrodes for picking up the electric current were attached to the channel. The device was tested by exciting an acoustic standing

**Table 1**

**Characteristics of a reasonably designed liquid sodium prime mover.**

Frequency	1000 Hz
Hot temperature	1000 K
Cold temperature	400 K
Mean pressure	200 bars
Dynamic pressure	198 bars
Plate spacing	0.0373 cm
Plate thickness	0.0280 cm
Distance of hot end from tube end	8.65 cm
Length of stack	8.0 cm
Average $Q_v$	300 W/cm <sup>2</sup>
Average $W$	55.1 W/cm <sup>2</sup>
$\eta$	0.184
$\eta/\eta_{\text{Carnot}}$	0.307

wave (by temporarily putting electric power *into* the magnetohydrodynamic converter!) and then letting the energy stored in the acoustic resonance flow through the converter into a resistive load across the electrodes. The efficiency-defined as the ratio of the measured electric energy delivered to the load to the calculated stored acoustic energy-is already quite high in this first prototype (Fig. 19) and a number of improvements are possible. From a technological point of view, it is very significant that the maximum efficiency is still reasonable in a magnetic field of only 0.9 tesla, suggesting that a permanent magnet is appropriate with a consequent simplification and decrease in weight.

The thermoacoustic prime mover tested had a single stack of molybdenum plates (Fig. 20) inside a straight half-wavelength tube. For this test the cold heat exchanger was filled with pressurized water at 125°C and the hot heat exchanger with heated sodium at various temperatures ranging from 440°C to 645°C. Although the test was preliminary, it was successful. The application of various temperature drops across the stack resulted in the data of Fig. 21 and, above a 350°C drop, in an obvious acoustic vibration of the entire assembly.

We obtained the rate of heat supplied to the engine  $\dot{Q}_h$  by monitoring the flow rate and the inlet and outlet temperatures of the sodium flowing through the hot heat exchanger. For a low temperature drop ( $\Delta T$ ) across the stack, the heat flow through the engine is due solely to the simple conduction of heat by the sodium, molybdenum, and stainless steel. However, for a  $\Delta T$  of around 400°C,  $\dot{Q}_h$  begins to increase dramatically>; above the value for simple conduction. This result agrees with the fact that acoustic oscillations at 906 hertz (Hz) were first detected at a  $\Delta T$  of 350°C. By the time  $\Delta T$  had reached 520°C the resonator was oscillating at high enough amplitude that the sound in the room was unpleasantly loud and the apparatus was vibrating strongly.

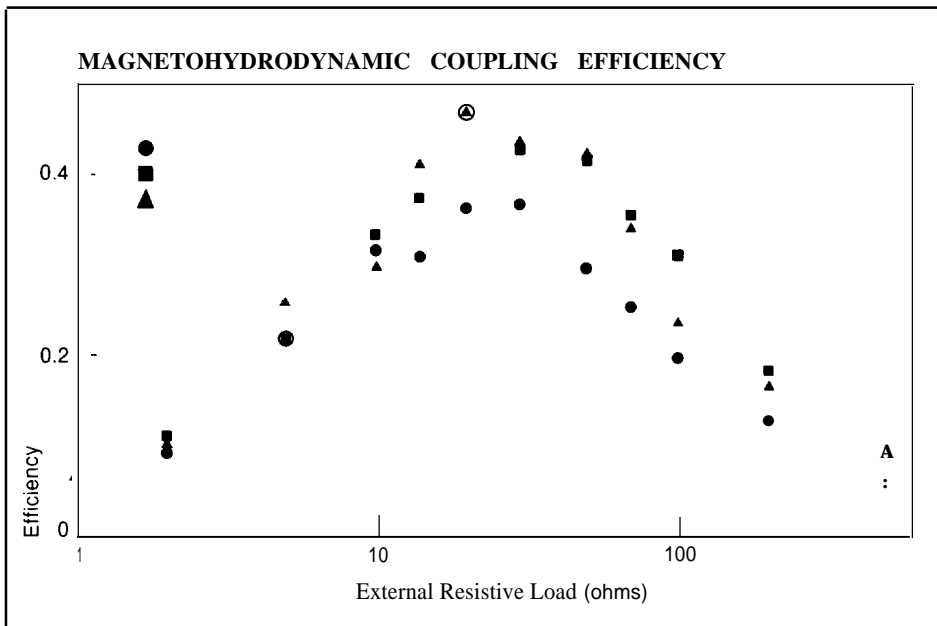
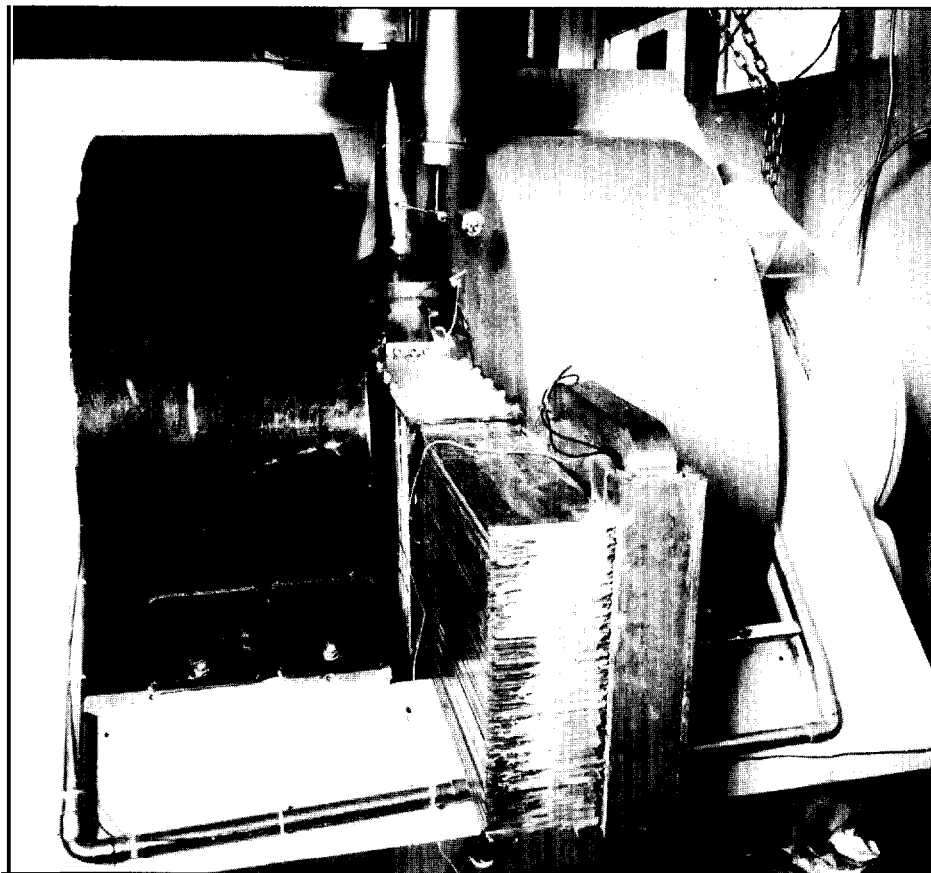
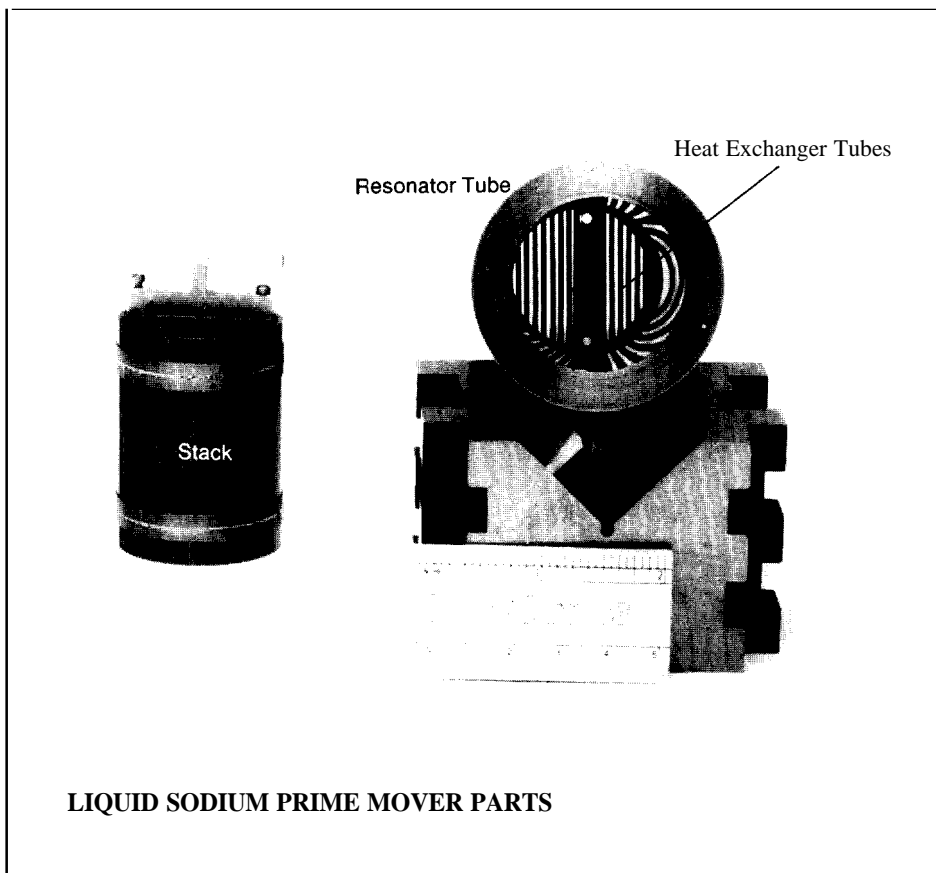


Fig. 19. These initial data demonstrate the efficiency with which acoustic energy in liquid sodium was converted to electric energy via magnetohydrodynamic coupling as a function of the resistance of an external load and for three different magnetic field strengths. In the apparatus used to obtain this data, the central rectangular channel

holding the liquid sodium is 1.2 cm thick in the direction of the magnetic field, 7.6 cm thick in the direction of electric current flow, and 31 cm long; however, only 20 cm of that length is actually in contact with the electrodes. The central channel is part of a 1-m-long acoustic resonator filled with liquid sodium at a temperature of 130°C. ▲



The magnetohydrodynamic converter used to test power coupling for the liquid sodium heat engine.



**Fig. 20.** Our first operating liquid sodium prime mover has a single stack of molybdenum plates (left) that were fabricated at Los Alamos from a solid rod using electric discharge machining. Plate thickness is 0.3 mm; spacing between plates is 0.38 mm; the length of the stack is only 5.2 cm so that the engine would oscillate at a reasonably low  $\Delta T$ . The transverse tubes of the two heat exchangers (one set can be seen at the end of the cylindrical section of

the resonator tube on the right) were made from stainless steel hypodermic needles. Hot liquid sodium at various temperatures ( $T_h$ ) is circulated through one heat exchanger and pressurized hot water ( $T_c = 125^\circ\text{C}$ ) through the other. The stack just fits inside the half-wavelength resonator tube, which has a length of 106 cm. The plates are positioned in the tube at about  $x = L/14$  from the end. The acoustic resonant frequency is 906 Hz.

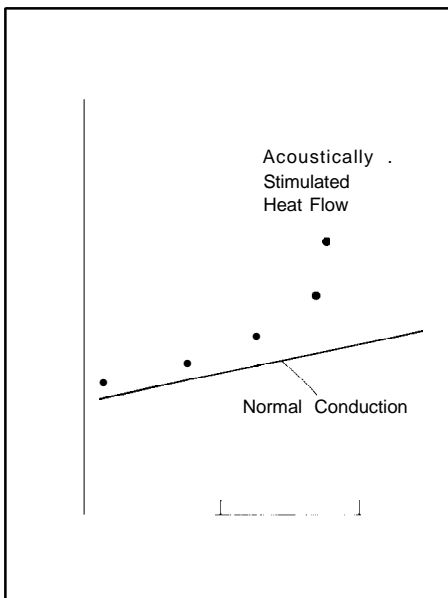


**Fig. 21.** The data shown here (dots) represent heat flow  $Q_h$  into the liquid sodium prime mover at the hot heat exchanger as a function of the temperature drop  $\Delta T$  across the stack, whereas the solid curve represents the calculated flow of heat due to conduction with no thermoacoustic effects. At low  $\Delta T$  heat flow is due to normal conduction across the stack. At high  $\Delta T$ , however, the sharp rise in  $Q_h$  is indicative of acoustically stimulated heat flow. ◀

There are some disagreements between the experimental results and our theoretical calculations. A calculation for the particular geometry and acoustic frequency of the device predicts that it should begin to oscillate at a  $\Delta T$  of  $260^\circ\text{C}$

rather than  $350^\circ\text{C}$ . We also expected a maximum  $\dot{Q}_h$  of 2000 watts at a  $\Delta T$  of  $520^\circ\text{C}$ , whereas the measured value was 2600 watts. We do not yet understand these quantitative disagreements but are extremely encouraged by the initial success of the engine.

**Molecular Natural Engines.** Heat engines of any sort transform energy between the random thermal motion of atoms and the coherent motion needed for useful work. The concepts of heat and temperature—implicit to the understanding of heat engines—are statistical in nature. Hence, for these variables to be well defined, a system must have large numbers of atoms. But what is the smallest system that will still allow us to apply these concepts?

If we take the error in statistical quantities in thermodynamics to be approximately the reciprocal of the square root of the number of degrees of freedom and if we assume for a heat engine that errors of a few per cent are tolerable, then only several hundred to a few thousand atoms are sufficient. Rather nice systems of this mesoscale size, consisting of large organic molecules, are common. Furthermore, such systems behave much like a purely classical collection of masses and springs.

Within such systems, nonlinear intermolecular potentials give rise to phenomena directly related to the thermal expansion needed for heat engines. Intramolecular and intermolecular interactions provide connections between regions of irrational energy that, if large enough, can be considered to be heat reservoirs. In other words, all the ingredients for an engine are present.

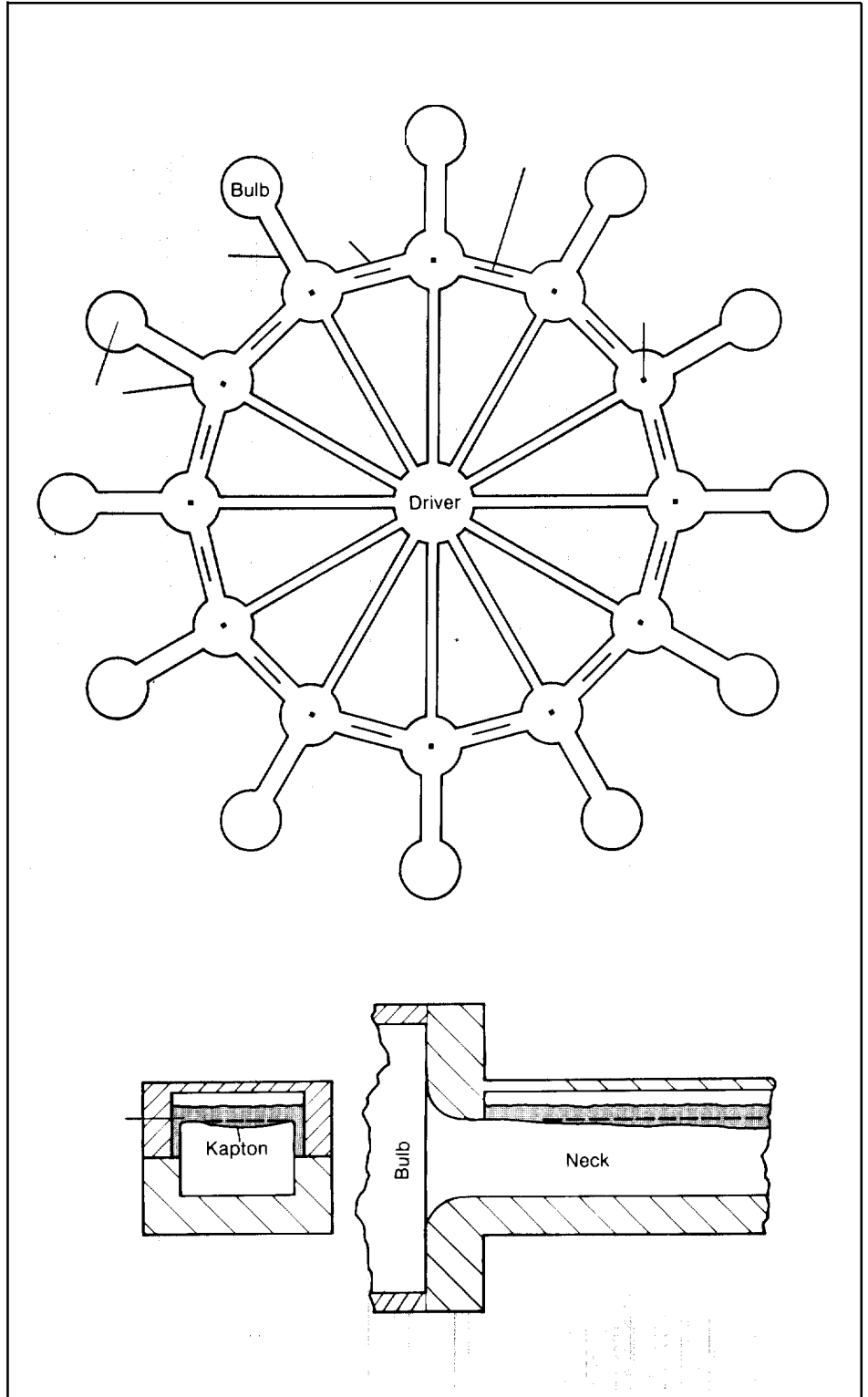
Do such engines then exist? And, if so, do they serve a useful function in nature, say perhaps as tiny engines in biochemical systems? Will the concepts of natural engines apply not only to these small sizes but also to the high frequencies associated with molecular vibrations?)

Heat pumping might occur in mesoscale systems if coherent vibratory motion

**Fig. 22. Localization of acoustic energy was studied by coupling twelve nonlinear Helmholtz resonators together in a ring and measuring the direction of heat flow with the thermoacoustic couples positioned in the coupling tubes and measuring the level of vibration in individual resonators with the pressure sensors. The construction of the neck of each resonator (see details below the dodecagon) introduces a nonlinearity because vibrating gas that rushes through the neck causes the Kapton to flex, altering the resonant frequency of that resonator. The entire system is driven by a loudspeaker at the center. ►**

can first be established and then survive long enough to have a significant effect. Also, if the concepts of temperature and temperature gradients are to be useful, then the mean free paths of the heat-carrying excitation should be small compared to the classical thermal penetration depth and to the size of the mesoscale object. Using an angular frequency of  $10^{11}$  Hz, we estimate the penetration depth to be about 14 angstroms. Hence, mesoscale objects perhaps 50 to 100 angstroms in size and vibrating at frequencies of order  $10^{10}$  Hz might be large enough and slow enough to be natural engines, providing their level of coherent excitation is high enough.

Rather than building an object of such small size, the same effects may be realized in a natural way via a concept from nonlinear science—the solitary wave. An acoustic heat engine with its stack of plates centered at a pressure anti node will pump heat from both ends of the stack toward the middle. If we alter this idea by using a continuous stack that has, owing to dispersive and nonlinear effects, a *localized*, or *solitary*, vibrational disturbance in the longitudinal direction, then heat is pumped from the wings to the center of the disturbance. Because the stack is continuous, the thermodynamic symmetry is not broken geometrically rather it is



broken dynamically. We call such a device a *nonlinear natural engine*. In principle, such a localized disturbance could be a vibrational excitation of a mesoscale object.

Localized waves in lower-dimensional vibrational systems have received a great deal of theoretical attention because of their potential application to biological processes. However, macroscopic modeling experiments in a water wave trough at the University of California, Los Angeles, have been very valuable in developing insight about solitary waves. (An outstanding example is the Wu-ton, a non-propagating soliton in water surface waves.) As a result, we decided to build an acoustical model that might give insight into how a coherently vibrating molecular system might behave. If such objects are indeed found to be real, we believe the field of potential applications will be much broader than just lower-dimensional systems.

Our apparatus, which we call the dodecagon, has been likened to a 12-element benzene ring. It consists of a circle of twelve coupled acoustic Helmholtz resonators with a nonlinear element included within each resonator (Fig. 22). We introduce the nonlinearity by building the resonator from two bulbs connected by a neck with a thin Kapton plastic film that flexes with changes in pressure. To prevent the neck from flapping at the acoustic frequency or its harmonics, we loaded the plastic film with oil.

According to one mathematical analysis, localization of energy can occur if the resonant frequency of any given resonator decreases as the amplitude increases. In our resonators, as the dynamic pressure of the acoustic wave increases, the velocity of fluid through the neck increases, which means, from Bernoulli's principle, that the average pressure there decreases. The Kapton neck then flexes inward, reducing the cross-sectional area and, thus, the resonant frequency (which is proportional to the square root of the area).

We installed a thermoacoustic couple in

each tube linking resonators to measure the direction of heat flow and also put a dynamic pressure sensor in each resonator to measure its level of vibration. The whole system was driven symmetrically from the center by an acoustic driver. When we drove the system at a frequency less than the low-amplitude resonance frequency, localization of energy *did* occur above a certain threshold amplitude. Further, heat was pumped toward the region of high amplitude. But the localization was stronger and occurred at a much lower drive amplitude than expected. This localization was also attended by a low-frequency modulation—typically at 1/11 or 1/12 of the drive frequency but often with components a factor of 100 or more times lower than the drive.

What happened? Our resonators performed as expected so far as alteration of the resonant frequency was concerned. However, we had unwittingly introduced a second set of vibrational systems into the experiment: plate-like vibrations on the Kapton-oil system. We believe that under suitable conditions the driver resonantly excites the Kapton-oil system and induces the film to make a hysteretic transition to a different geometry that facilitates the localization.

Our acoustical model experiments have been helpful in inspiring thought on molecular-scale or mesoscale systems. Localization of energy and heat pumping *did* occur. More important, though, attending and preceding the localization, we observed behavior that changed on an entirely different time scale than the acoustic phenomenon.

We conjecture that in molecular and mesoscale systems it is important to have two or more interacting, or coupled, "fields." These coupled fields could be some of the normal optical vibrational modes of a molecular system. In particular, torsional or vibrational modes of motion are almost certainly coupled nonlinearly with the longitudinal modes of motion. We expect a time-dependent confirmational change, say in the long-

itudinal field, to attend localization of vibrational energy. The fundamental molecular vibrational frequencies are of the order of  $10^{12}$  Hz or greater, but a time-dependent confirmational change in the longitudinal field could beat a much lower frequency—possibly low enough to create natural engine effects. These conjectures have motivated us to begin experimental work with a number of other collaborators on the general question of the localization of vibrational energy in materials. This is a case where we think we know what we are looking for, but we don't know what we will find.

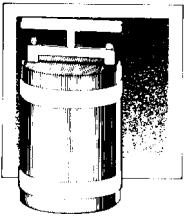
Thus, whether shaking loudly in the laboratory or, perhaps, vibrating soundlessly in a molecule, natural engines may be a widespread phenomenon of general importance. Not only are natural engines simple, they use a necessary thermodynamic evil—irreversibilities—as a positive feature of the engine. We hope an understanding of these concepts will serve mankind well in his quest for appropriate engines and will help us to comprehend better the behavior of molecular vibrational systems. ■

## Further Reading

John Wheatley, T. Hofler, G. W. Swift, and A. Migliori. 1985. Understanding some simple phenomena in thermoacoustics with applications to acoustical heat engines. *American Journal of Physics* 53:147.

J. C. Wheatley, T. Hofler, G. W. Swift, and A. Migliori, 1983. An intrinsically irreversible thermoacoustic heat engine. *Journal of the Acoustic Society of America* 74:153.

G. W. Swift, A. Migliori, T. Hofler, and John Wheatley. 1985. Theory and calculations for an intrinsically irreversible acoustic prime mover using liquid sodium as primary working fluid. *Journal of the Acoustic Society of America* 78:767.



# The Liquid Propylene Engine

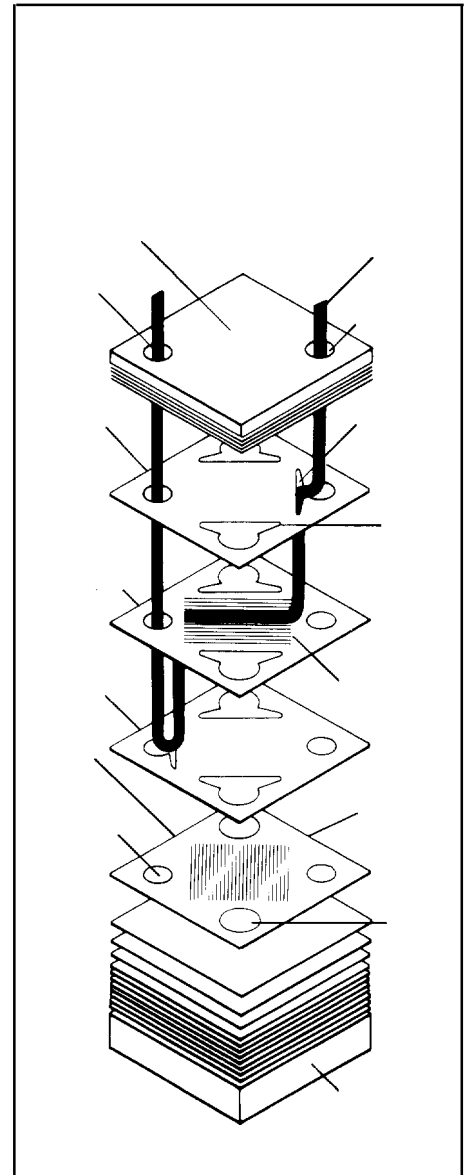
An ideal use of geothermal energy is to warm buildings by extracting heat from ground water at temperatures of only about 10°C. This application involves the pumping of large amounts of heat across small temperature differences (of the order of 30°C). An efficient way to effect such heat transfer is from one liquid to another. As a result, a heat pump that appears well suited for this purpose is a conventional reciprocating heat engine using a *liquid* for a working substance.

We have been studying just such an engine—a Stirling engine that uses liquid propylene as its working fluid. Our discussion of this device will both contrast the simplicity of natural engines with the complexity of more traditional engines and, more important, will introduce the use of a liquid as a thermodynamic working substance. (The section in the main article called “The Liquid Sodium Acoustic Engine” discusses a *natural* heat engine that uses a liquid as its primary thermodynamic medium.)

It is a common misconception that liquids behave much like an idealized hydraulic fluid, with density independent of temperature and pressure. In fact, especially near the critical point (where the liquid and gaseous phases become indistinguishable), a typical real liquid is somewhat compressible, has a large thermal expansion coefficient (comparable to or larger than that of an ideal gas!), and has other attractive thermophysical proper-

**Fig. 1. In this propylene-to-water heat exchanger, made up of a stack of hundreds of stainless steel sheets copper-brazed together at Los Alamos, the propylene flows in at the top right of the stack and across through the propylene manifolds and channels, then moves up and out through the other propylene duct. The arrow in the figure traces the path through just one of the sets of channels and manifolds; similar flow occurs through the other, lower propylene channels and manifolds. At the same time, water flows in and up through one water duct and across the stack (but through alternate sets of plates and across the plates in a direction perpendicular to the corresponding propylene flow) until it returns, exiting through the other water duct. Because of the intimate thermal contact between fluid and stainless steel, heat can be transferred at a rate of 230 W/°C. ►**

ties. These facts were first appreciated by John Malone, who in the 1920s built several Stirling prime movers that used liquid water with pressures as high as 700 bars as the working substance. We chose liquid propylene (C<sub>3</sub>H<sub>6</sub>) for our work because its critical temperature is just above room temperature and its Prandtl number (which can be thought of as a measure of the material’s viscous losses in relation to its thermal transport capacity) is lower



than that of other fluids with similar critical temperatures,

A major advantage of a liquid working substance is that liquids have a very large heat capacity per unit volume compared to gases, making it possible to build efficient and compact heat exchangers and regenerators. This point is illustrated by the compact propylene-to-water heat exchanger we have developed for our engine (Fig. 1). The exchanger is made of hun-



**Fig. 2.** The heat engine shown here consists of four Stirling engines of the Rider form operating from a common crankshaft but phased 90 degrees apart. The working medium is liquid propylene, and heat exchange between water and the propylene takes place in the stainless-steel exchangers depicted in Fig. 1.4

photograph, when contrasted with photographs of natural engines (see the main article) is nevertheless a dramatic representation of the complex of a more conventional reciprocating engine.

In its heat-pump mode, our engine uses work supplied by an electric motor to transfer heat from a source at or below room temperature to a heat sink consisting of flowing water at or above room temperature. For convenient measurement, the low-temperature source is an electric heater. Mean pressure, oscillating pressure amplitude, volumetric displacement, shaft rotation frequency  $f$ , and hot and cold temperatures are all independently controllable. We can measure both the rate at which heat is pumped away from the heat source  $Q$  and the shaft torque  $\tau$ , the latter giving us shaft power  $\dot{W} = 2\pi f\tau$ .

In addition, our laboratory engine has valves that quickly change it from the ordinary heat-pump configuration to one in which there is no flow of propylene through the regenerators and heat exchangers, even though crankshaft and piston motion, pressure amplitudes, temperatures, and so forth remain the same. This feature allows us to accurately measure just the torque *difference*  $\Delta\tau$  required to pump the heat, with the background torques due to bearing and seal friction, piston blowby, and the like eliminated.

Large amounts of heat can be pumped by the engine (Fig. 3a)—around 1300 watts at a crankshaft rotation frequency of 4.5 Hz—and the data points match very well curves predicted from theory for the particular geometry of the engine and for the use of propylene as the working fluid.

dreds of chemically milled stainless-steel sheets copper brazed together (several of the individual plates are shown on the cover). Although the exchanger (4 by 4 by 9 centimeters in size) entrains only a few cubic centimeters of propylene, it transfers heat between the two fluid streams at a rate of 230 watts per °C with only a few watts of power required to pump the fluids through the exchanger.

Another advantage of a liquid working substance is that liquids are typically much less compressible than gases. Thus the large pressure amplitudes needed to pump large amounts of heat can be achieved with only small displacements of a piston, even for a substantial volume of entrained liquid in the thermal elements.

Because of this quality it is possible to build a high-power engine that uses a short stroke, making the mechanical elements very efficient without compromising on the size and efficiency of the thermal elements.

Our Laboratory-scale liquid-propylene Stirling engine (Fig. 2) uses the same configuration of parts shown in Fig. 3 of the main article (the Rider form of the Stirling engine), except that we have *four* such assemblies. These assemblies operate from a common crankshaft and are mechanically phased 90 degrees apart so that the shaft torque oscillations are minimized, eliminating the need for a big flywheel. Although much of the wiring in Fig. 2 is for diagnostic purposes, the

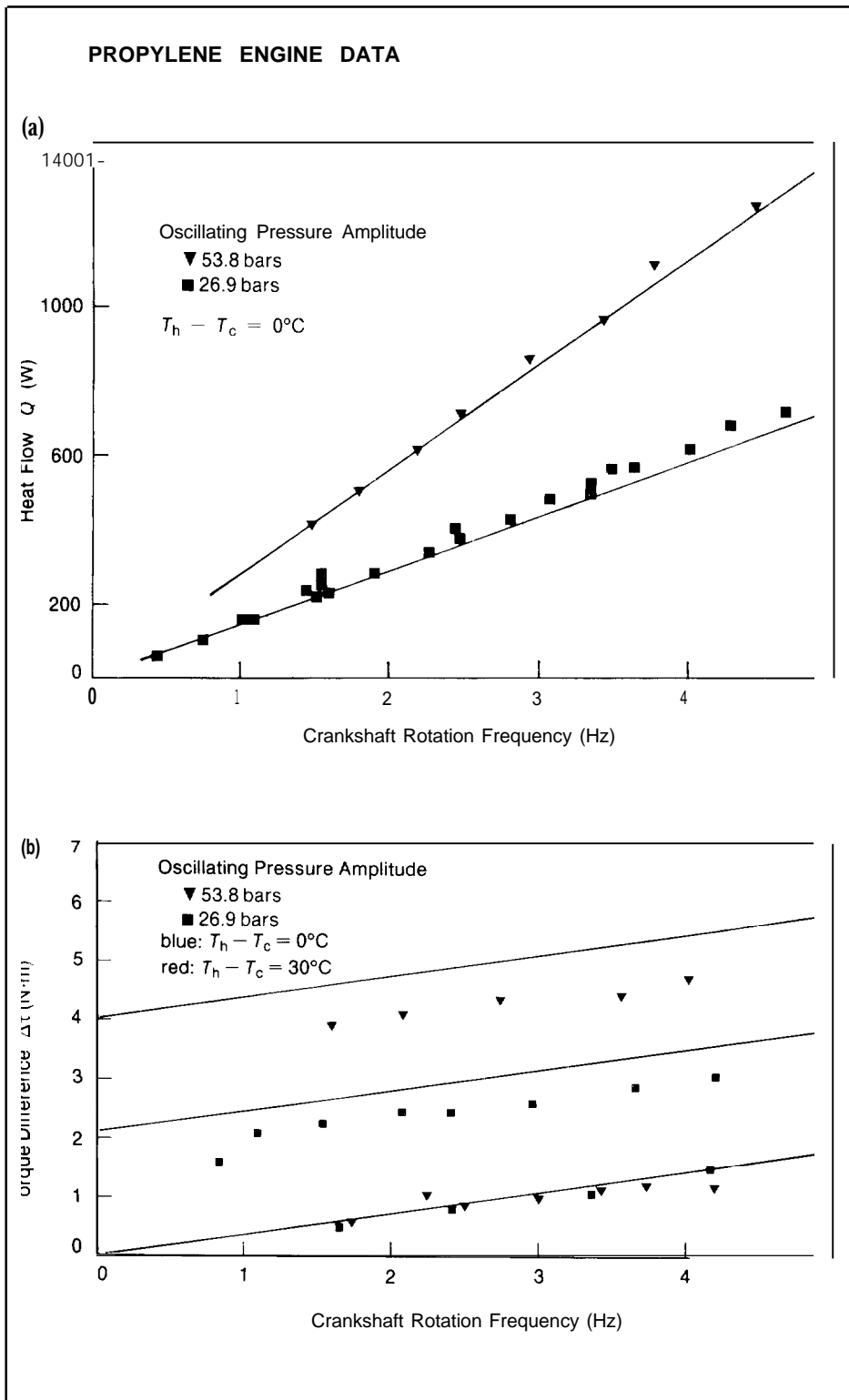


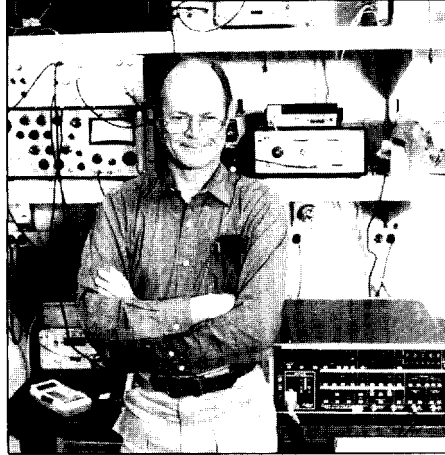
Fig. 3. (a) The rate at which the propylene engine pumps heat  $Q$  as a function of crankshaft rotation frequency  $f$  at two different oscillating pressure amplitudes agrees very well with theoretical curves predicted from the physical properties of propylene and the geometry of the engine. (b) The torque difference  $\Delta\tau$ , here also plotted as a function of  $f$ , is just that part of the torque needed to pump the heat. In both graphs the blue data points represent no temperature difference across the regenerators, whereas the red data points represent a  $30^\circ\text{C}$  difference. ◀

The lines drawn on Fig. 3b represent the torque required by an engine with the Carnot efficiency to pump the observed amount of heat added to the torque associated with just the viscous losses of pushing the fluid through the regenerators and heat exchangers. Our measured torque differences agree well with these theoretical curves.

Our laboratory engine is very far from a practical, economically useful device. Its scale and most of its design are appropriate for experimental measurements and for the understanding of principles. not for optimized efficiency or low manufacturing or operating costs in a specific application. But, as expected, we are learning that liquids are good heat engine working substances, Liquid engines may ultimately be of great technological importance.

We are also learning much about the practical details of the use of liquids in engines. For example, we suspect that the next logical step in the development of practical liquid engines is to abandon the reciprocating Stirling engine entirely. Instead, we would use the liquid in, say, a Brayton engine with rotary compressors and expanders. Such a configuration would reduce losses from such things as bearing and seal friction that, until now, we have regarded as quite uninteresting. ■

**John C. Wheatley** (1927-1986) joined Los Alamos in 1981. During his tenure here, he performed experiment; on novel heat engines and on the fundamentals of thermal and statistical physics. He received his B.S. in electrical engineering in 1947 from the University of Colorado and his Ph.D. in physics in 1952 from the University of Pittsburgh. He was elected a member of the National Academy of Sciences in 1975 and appointed to the Academy of Finland in 1980. His many honors include the two top awards given by the low-temperature physics community: the Simon Memorial Prize and the Fritz London Memorial Award. At the time of his death, he was the first joint Fellow of the University, of California, Los Angeles, and Los Alamos National Laboratory



**Albert Migliori** earned his B.S. in 1968 from Carnegie-htellon University and his Ph.D. in physics in 1973 from the University of Illinois, where he studied superconducting thin films. He then joined Los Alamos as a pos-doctoral fellow and studied high-field and self-field behavior of hard type II superconductors. In 1975 he was awarded a National Science Foundation Fellowship to study internal and surface magnetic fields in current-carrying superconductors with the Mossbauer effect. In 1976 he became a staff member of the Condensed Matter and Thermal Physics Group.



**Gregory W. Swift** is a staff member in the Condensed Matter and Thermal Physics Group, where he has been working on novel heat engines, acoustics, and superfluid helium-3 since 1981. He received his B.S. in physics and mathematics from the University, of Nebraska and his Ph.D. in physics from the University of California, Berkeley. From 1983 to 1985 he held an Oppenheimer Fellowship at Los Alamos.

